Tumor cells can follow distinct evolutionary paths to become resistant to epidermal growth factor receptor inhibition

Title: Tumor cells can follow distinct evolutionary paths to become resistant to epidermal growth factor receptor inhibition

Authors: Aaron N Hata[1,2,*], Matthew J Niederst[1,2,*], Hannah L Archibald[1], Maria Gomez-Caraballo[1], Faria M Siddiqui[1], Hillary E Mulvey[1], Yosef Maruvka[3], Fei Ji[4], Hyo-eun C Bhang[5], Viveksagar K Radhakrishna[5], Giulia Siravegna[6,7], Haichuan Hu[1], Sana Raoof[1], Elizabeth Lockerman[1], Anuj Kalsy[1], Dana Lee[1], Celina L Keating[5], David A Ruddy[5], Leah J Damon[1], Adam S Crystal[1], Carlotta Costa[1], Zofia Piotrowska[1,2], Alberto Bardelli[6,7], Anthony J. Iafrate[8], Ruslan Sadreyev[4], Frank Stegmeier[5], Gad Getz[1,3], Lecia V Sequist[1,2], Anthony C Faber[9], Jeffrey A Engelman[1,2]

Affiliations:

[1]Massachusetts General Hospital Cancer Center, Charlestown, MA, USA

[2]Department of Medicine, Harvard Medical School, Boston, MA, USA

[3]Broad Institute of MIT and Harvard, Cambridge, MA, USA.

[4]Department of Molecular Biology, Massachusetts General Hospital, Boston, MA, USA.

[5]Oncology Disease Area, Novartis Institutes for Biomedical Research, Cambridge, MA, USA.

[6]University of Torino, Department of Oncology, Torino, Italy.

[7]Candiolo Cancer Institute - Fondazione Piemontese per l'Oncologia (FPO), Istituto di Ricovero e Cura a Carattere Scientifico (IRCCS), Candiolo, Torino, Italy.

[8]Department of Pathology, Massachusetts General Hospital, Boston, MA, USA.

[9]Virginia Commonwealth University Philips Institute for Oral Health Research, School of Dentistry and Massey Cancer Center, Richmond, VA, USA

[*]These authors contributed equally to this work

Address correspondence to: Jeffrey A. Engelman, Massachusetts General Hospital Cancer Center, Building 149, 13th St, Boston, Massachusetts 02129, USA. Phone: 617.724.7298; Fax: 617.724.9648; E-mail: jengelman@partners.org.

Abstract

Acquired drug resistance to targeted cancer therapies remains a significant clinical problem. Although mechanisms of acquired resistance of EGFR mutant non-small cell lung cancers to EGFR inhibitors have been identified, little is known about how resistant clones evolve during drug therapy. Herein, we observe that acquired resistance caused by the T790M gatekeeper mutation, which occurs in 50-60% of patients with acquired resistance to EGFR inhibitor therapy, can occur by either selection of pre-existing T790M clones or via evolution of T790M-negative drug tolerant cells that develop the mutation during drug treatment. Additionally, the path to resistance impacts the biology of the resistant clone, as those that evolved from drug tolerant cells have a diminished apoptotic response to third generation EGFR inhibitors that target T790M EGFR and can be sensitized by BCL-XL inhibitors. This observation is corroborated in cell cultures derived directly from resistant patient biopsies. These findings provide evidence that clinically relevant drug resistant cancer cells can both pre-exist and evolve from drug tolerant cells, and point to new therapeutic opportunities to prevent or overcome resistance in the clinic.

Introduction

Despite the success of targeted cancer therapies, the duration of clinical response is limited by the inevitable development of acquired drug resistance, as in the case of *EGFR* mutant non-small cell lung cancers (NSCLC) treated with EGFR inhibitor therapy[1-3]. Although molecular mechanisms of acquired resistance to EGFR inhibitors have been identified[4-6], little is known about how resistant clones evolve during drug therapy. In some cases, clones with clinically validated genetic resistance mechanisms may exist prior to drug exposure that may simply be selected by treatment[7-10]. Alternatively, it has been hypothesized that drug tolerant (or "persister") cells without *bona fide* resistance mechanisms may survive initial drug treatment by epigenetic adaptations[11-13], and undergo further evolution over time to acquire validated genetic resistance mechanisms (Supplementary Fig. 1). Although this would have immediate implications for new therapeutic strategies to prevent resistance, there has not been any direct evidence that drug tolerant cells can undergo such evolution.

To better understand the evolution of acquired resistance, we studied the development of resistance caused by the T790M gatekeeper mutation, which occurs in 50-60% of patients with acquired resistance to EGFR inhibitor therapy[4]. By monitoring the development of large numbers of resistant clones in parallel, we were able to identify temporal patterns that reflected emergence of pre-existing resistant T790M clones as well as de novo acquisition of the T790M mutation within initially T790M-negative drug tolerant cells. Moreover, the path to resistance impacts the biology of the resistant clone, as those that evolved from drug tolerant cells bear epigenetic hallmarks of the drug tolerant state and have a diminished apoptotic response to third generation EGFR inhibitors that target T790M EGFR. These findings provide evidence that drug

resistant cancer cells bearing the identical clinically relevant genetic resistance mechanism can both pre-exist and evolve from drug tolerant cells, and suggest that cancer cells that survive initial therapy may serve as an important reservoir from which acquired resistance can emerge in the clinic.

Results

Gefitinib resistant PC9 cells that harbor T790M have differential apoptotic response to third generation EGFR inhibitor treatment

We previously cultured sensitive EGFR mutant NSCLC PC9 cells in escalating concentrations of the EGFR inhibitor, gefitinib, until resistant clones emerged[14]. Notably, in two resistant cell lines, PC9-GR2 and PC9-GR3, there was a marked difference in the time required to develop resistance, with the GR2 and GR3 lines developing in 6 and 24 weeks, respectively (Fig. 1a). Treatment with the third generation irreversible EGFR inhibitor WZ4002[15] suppressed EGFR phosphorylation and downstream MEK and PI3K signaling and induced cell cycle arrest in both resistant cell lines (Supplementary Fig. 2a-c). However, WZ4002 induced robust mitochondrial depolarization and subsequent apoptosis only in the PC9-GR2 cells (Supplementary Fig. 2d, Fig. 1b). Analysis of the expression of BCL-2 family genes, which regulate the mitochondrial apoptotic response induced by MEK/ERK and PI3K/AKT signaling pathways[16], revealed that PC9-GR3 cells had diminished upregulation of BIM (Supplementary Fig 2e, f), a key mediator of apoptosis in EGFR mutant NSCLC[17-20]. Similarly, induction of BIM protein levels after drug treatment were significantly lower in PC9-GR3 cells compared with PC9-GR2 and parental cells (Supplementary Fig. 2g). Consistent with the differential levels of apoptosis following treatment with WZ4002, treatment led to regression of PC9-GR2 but not GR3 cells in vitro (Fig. 1c,

Supplementary Fig. 2h) and xenograft tumors in vivo despite comparable inhibition of EGFR and ERK phosphorylation (Fig. 1d, Supplementary Fig. 3a).

Early emerging T790M resistant clones derive from pre-existing T790M cells

The variable time to resistance led us to question whether the GR2 and GR3 cells may have developed T790M via different mechanisms (i.e. pre-existing versus drug tolerant evolution (Supplementary Fig. 1)). To explore this possibility, we cultured over 1,200 small pools (~5,000 cells each) of parental PC9 cells in the presence of gefitinib and monitored for emergence of resistant clones. After two weeks of drug exposure, 5-10% of the wells contained a rapidly growing resistant colony (Fig. 2a), whereas the other wells contained a small number of surviving drug tolerant cells similar to those described previously by Settleman and colleagues[11]. Allele specific quantitative PCR revealed that all "early" resistant colonies examined (N=50) harbored the T790M mutation (Supplementary Fig. 4a), and all were sensitive to WZ4002 but not gefitinib (Fig. 2b). Treatment of PC9 pools with WZ4002 yielded drug tolerant cells but completely suppressed emergence of the early T790M colonies (Fig. 2c). Conversely, treatment of PC9 pools with gefitinib + the IGFR inhibitor NVP-AEW541, which was previously shown to abrogate the survival of PC9 drug tolerant cells[11], eliminated drug tolerant cells without affecting the emergence of early T790M resistant clones. These results demonstrate that the early T790M resistant clones emerged independently from drug tolerant cells.

Direct detection of genetically distinct rare sub-populations using currently available standard next-generation sequencing is limited to allelic frequencies of approximately 0.1%[21], whereas droplet digital PCR has a sensitivity of 0.01-0.005%[22]. In our PC9 parental cell line, we

estimated that approximately 1 out of 25,000-50,000 cells harbor a T790M allele prior to treatment (see Methods for calculation). Because PC9 cells carry 8-10 copies of EGFR (Supplementary Fig. 4b), and only one T790M allele is required to confer resistance (Supplementary Fig. 4c-d), direct detection of the pre-existing T790M clones in our parental PC9 population would necessitate a sensitivity at least an order of magnitude beyond what is routinely achievable.

To overcome these limitations, Stegmeier and colleagues recently reported a high-complexity DNA barcode library (ClonTracer) designed to track the evolution of pre-existing resistant clones too rare to be detected by direct approaches[8]. In this system, when a population of barcoded cells is made resistant to drug, enrichment of a shared set of barcodes between multiple replicates indicates emergence of pre-existing resistant clones. We utilized the ClonTracer lentiviral barcode library to determine whether the early resistant T790M clones were derived from cells with pre-existing T790M mutation. We transduced 1-2 million PC9 cells with the lentiviral Clontracer library, expanded the cells and split the cells (CT-A) into multiple biological replicates with approximately 10-fold representation of barcode complexity (Supplementary Fig. 5a). Cells were treated with 300 nM gefitinib, and consistent with our prior experiments, rapidly proliferating early resistant clones were observed. These clones were T790M positive (Supplementary Fig. 5b), and we observed a highly consistent number of unique barcodes enriched in each replicate (Fig. 2d, Supplementary Fig. 5c). Approximately 90% of enriched barcodes in each sample were shared by at least two other replicates and over 50% were shared by all five replicates (Fig. 2e, Supplementary Fig. 5d). Notably, the most highly shared barcodes were also the most highly enriched. We repeated the entire experiment with two additional,

independently barcoded PC9 populations (CT-B and CT-C) that yielded the same results (Fig 2e, Supplementary Fig. 5b-d). These results confirm that the early resistant T790M clones were derived from pre-existing T790M mutant cells that were selected during gefitinib treatment.

Late emerging T790M resistant clones derive from drug tolerant cells

To determine whether T790M could also evolve during treatment from initially T790M-negative drug tolerant cells, we cultured 16 PC9 drug tolerant cell pools with no evidence of early resistant clones in the presence of gefitinib until they had reached numbers sufficient for genotyping and drug sensitivity testing, which required 12-16 weeks. These pools remained partially resistant to both gefitinib and WZ4002, and T790M allele-specific PCR was negative, indicating non-T790M mediated resistance (Fig. 3a, Supplementary Fig. 6a). These cells were further cultured in gefitinib until fully resistant (20-40 weeks cumulative drug exposure) and five of the 16 resistant pools acquired T790M and demonstrated increased sensitivity to WZ4002 (Fig. 3a, Supplementary Fig. 6b). To gain a better understanding of the kinetics of evolution of T790M resistance in these cells, we examined additional intermediate time points during the development of the original PC9-GR3 resistant line and several of the late T790M clones. For the PC9-GR3 line, T790M was first detected at 22 weeks, at a fraction of 6% of the total cell population, and within one month had overtaken the population as the dominant clone (Supplementary Fig. 6c-d, Supplementary Fig. 4d). In the other three cases examined, a minority T790M clone was observed at 34, 43 and 47 weeks, and by one month later had overtaken the population as the dominant clone (Supplementary Fig. 6d). Thus, these results suggest that the T790M resistance mutation can develop *de novo* in drug tolerant cells during the course of prolonged exposure to EGFR inhibition.

Resistant cells that remained T790M-negative were subjected to clinical multiplexed genetic analysis that assessed for single nucleotide variants and insertions/deletions in 39 cancer-related genes[23]. Notably, these T790M-negative resistant cells were found to have acquired mutations in NRAS, KRAS, BRAF and RET (Supplementary Table 1), albeit at low allele frequencies suggesting mixed clonal populations. We did not observe MET or HER2 amplification, and one resistant line had low-level KRAS amplification in addition to a KRAS mutation (Supplementary Fig. 7a) in addition to a KRAS mutation. Although some of these mutations have been previously observed in PC9 cells and in resistant EGFR mutant NSCLC tumors by others[24,25], the significance of these particular mutations driving resistance in the clinic is unclear. Nonetheless, these results suggest that drug tolerant cells have the potential to develop both T790M and non-T790M mechanisms of resistance, which may contribute to the heterogeneity of acquired resistance observed in the clinic[4,26].

To further convince ourselves that T790M could evolve during treatment from initially T790M-negative drug tolerant cells, we established PC9 sub-clones derived from single cells to eliminate pre-existing T790M cells. Indeed, in ten independent clones derived from single cells, no early T790M colonies emerged after two weeks of gefitinib treatment (Supplementary Fig. 8a) in contrast to the parental PC9 cells which harbored pre-existing T790M cells (Fig. 2a). We then cultured 14 pools (5,000 cells each) from single cell-derived sub-clone A (Supplementary Fig. 8a) in gefitinib up to 40 weeks until fully resistant cells emerged. Eight acquired T790M and six remained T790M-negative (Fig. 3b, Supplementary Fig. 8b). Similarly, three additional clones (B-D) were cultured in gefitinib for several months, and all developed T790M clones (data not

shown). To provide statistical evidence that these late T790M clones did not derive from undetected pre-existing T790M cells, we spiked single RFP-labeled T790M PC9 cells into pools of unlabeled sub-clones A-D (5,000 cells), and measured the kinetics of emergence of the resistant clone. As shown in Supplementary Figure 8c , over a ten week time period, all resistant clones were derived from RFP-positive T790M cells, with the majority emerging within the first two weeks. From this, we derived a cumulative density function (CDF) describing the probability of detecting the emergence of pre-existing T790M resistant cells as a function of time (Supplementary Fig. 8d-e). Since none of the single cell-derived sub-clones gave rise to T790M clones at 2 weeks (Supplementary Fig. 8a), the CDF determines that the probability that the late emerging T790M clones in clones A-D derived from undetected pre-existing T790M cells is 0.006 (see Supplementary Fig. 8 legend for calculation). Taken together, these results confirm that T790M acquired resistance can evolve from initially T790M-negative drug tolerant cells.

Considering the time scale and cell population sizes of our experiments, we were initially surprised that the T790M mutation could arise in these drug tolerant cells. Taking into account reasonable estimates of mutation and cell division rates, we mathematically modeled d*e novo* acquisition of T790M in drug tolerant cells. We applied a simple branching model, similar to Chmielecki et al.[27], estimating the birth rate of drug tolerant cells calculated from previously reported single cell imaging experiments of PC9 cells treated with erlotinib[28]. The growth rate and the initial population size of the drug tolerant PC9 cells were determined by experimentally measuring the proliferation of drug tolerant PC9 cell pools over time (N = 300, Supplementary Fig. 9a). We both solved analytically (SI) and simulated this model, and there was very close agreement between the results (Supplementary Fig 9b). In Figure 3c, we display the fraction of

drug tolerant pools predicted to acquire T790M by 16 weeks of gefitinib treatment for a range of values of mutation and division rates. This fraction grows linearly with the initial population size, division and mutation rates, and exponentially with the growth rate and time. Additionally, we calculated the fraction of drug tolerant pools predicted to acquire T790M as a function of time using a reasonable set of parameters (Fig. 3d). The mathematical model did predict emergence of T790M over a time period corresponding to several months. To assess the model experimentally, we treated 484 pools of drug tolerant 5000 PC9 cells derived from the single-cell clones with gefitinib for 16 weeks at which point 203 had reached sufficient numbers to genotype (Supplementary Fig. 9b). Three were found to be T790M positive (1.5%), which is in remarkable agreement with the modeling results.

To examine whether T790M can evolve from drug tolerant cells in other EGFR mutant NSCLC models, we examined MGH119 cells that were previously derived in our laboratory from a treatment naïve EGFR mutant NSCLC patient[14]. MGH119 cells were cultured in gefitinib until resistant, and two independent T790M resistant lines (GR1, GR2) developed after 5-6 months. To determine if T790M cells pre-exist in this model, we treated MGH119 cell pools with gefitinib for three weeks, but no early resistant colonies were observed (Supplementary Fig. 10a). In contrast, when we simulated the presence of pre-existing T790M cells by introducing RFP-labeled MGH119-GR1 cells into MGH119 parental cells, emerging gefitinib resistant RFP-positive colonies were detectable starting at 2-3 weeks (Supplementary Fig 108b). At 10 weeks, only RFP-positive resistant clones were observed. These results suggest that the MGH119 cell line does not harbor pre-existing T790M cells, and that the MGH119-GR1 and GR2 resistant cells arose from drug tolerant cells by acquiring T790M during drug treatment.

Late T790M resistant cells bear hallmarks of evolving from drug tolerant state

We next sought to determine if late T790M resistant cells exhibited molecular evidence of having evolved from the drug tolerant state, using RNA-Seq to compared the transcriptional profiles of PC9 drug tolerant cells with PC9-GR3, PC9-GR2 and PC9 parental cells (Supplementary Fig. 11a). Principal component analysis of global expressed mRNA transcripts at baseline and after EGFR inhibitor treatment revealed that four distinct clusters, The late T790M PC9-GR3 cells clustered with drug tolerant cells, and the T790M PC9-GR2 cells clustered with the parental PC9 cells (Fig. 3e). Whereas as PC1 primarily differentiated between baseline and drug treated samples, PC2 segregated late T790M PC9-GR3 and drug tolerant cells from early T790M PC9-GR2 and parental cells (Supplementary Fig. 11b). Gene set enrichment analysis revealed upregulation of genes related to epithelial-to-mesenchymal transformation in drug tolerant/PC9-GR3 cells relative to parental PC9-GR2/parental cells, which has been linked to acquired resistance to EGFR inhibitor therapy in the clinic[4]. Taken together, these results demonstrate that the late emerging T790M PC9-GR3 cells share a transcriptional profile most similar to drug tolerant cells. This further supports the model that the late T790M resistant cells evolved from drug tolerant cells (Fig. 3f) and suggests that molecular features of the drug tolerant state may be maintained even after acquisition of T790M.

Late T790M resistant cells have decreased apoptotic response to 3rd generation EGFR inhibitor therapy

By definition, evasion of drug-induced apoptosis in the presence of EGFR inhibition is a characteristic feature of drug tolerant cells (Supplementary Fig. 12a-b). Since late T790M

resistant cells evolved from drug tolerant cells and continue to share a similar mRNA expression profile (Fig. 3e), we reasoned that they might also exhibit reduced apoptotic sensitivity to subsequent EGFR inhibition. Similar to PC9-GR3 cells (Fig. 1b), late T790M resistant PC9 clones that emerged from drug tolerant cells had a reduced apoptotic response to WZ4002 treatment compared to early T790M resistant clones that derived from pre-existing cells (Fig. 4a). Moreover, when we induced expression of T790M EGFR in drug tolerant cells, the T790M resistant clones that grew out had reduced apoptotic sensitivity to WZ4002 (Supplementary Fig. 13a-b). MGH119-GR1 and GR2 cells, which developed T790M late consistent with evolution from drug tolerant cells, also exhibited reduced apoptotic response to WZ4002 relative to MGH119 parental cells and MGH119 cells in which we introduced T790M EGFR by lentiviral expression (Fig. 4b, Supplementary Fig. 13c). These results demonstrate that T790M resistant cells that evolve during drug treatment have reduced dependence on EGFR activation for survival compared to pre-existing T790M cells, consistent with the notion that these cells evolved from drug tolerant cells that are by definition less sensitive to EGFR inhibition than those that underwent apoptosis upon initial treatment.

To investigate the clinical implications of the laboratory-derived acquired resistance models, we examined cell lines derived from *EGFR* mutant NSCLC patient tumors at the time of clinical progression due to T790M acquired resistance[14] (Supplementary Table 2). Three cells lines were exquisitely sensitive to WZ4002, whereas four had a diminished apoptotic response and increased in vitro survival (Fig. 4c-d). In vivo sensitivity of MGH141 and MGH134 xenograft tumors mirrored the in vitro response, with the low apoptosis MGH134 cell line xenografts failing to undergo tumor regression (Fig. 4e) despite suppression of EGFR and ERK signaling

(Supplementary Fig. 3b). Intriguingly, the least sensitive cell lines corresponded to patients with the longest duration of response to first line EGFR inhibitor therapy prior to development of drug resistance (Fig. 4f), raising the possibility that these low-apoptotic resistant cells evolved from drug tolerant cells.

These results raise the possibility that resistant cancers in which T790M originates during therapy may have a reduced apoptotic sensitivity to third generation EGFR inhibitors that are currently being evaluated in the clinic[29-31]. Therefore, we sought to identify therapeutic strategies that could enhance the apoptotic response to third generation EGFR inhibitors. Recently, we reported a drug screening strategy for identifying effective drug combinations for cancers with acquired resistance to targeted therapies[14]. Because this screen was focused on overcoming bypass resistance mechanisms, effective drug combinations were identified based on a shift in GI50. However, we noted that the decrease in apoptosis in our models was most clearly reflected by a change in Emax (Supplementary Fig. 14). Therefore we reanalyzed the screen data for three low apoptosis T790M patient-derived cell lines (MGH134, MGH157, MGH125) to identify drugs that increased Emax when combined with WZ4002. Additionally, we performed the identical drug screen on PC9-GR3 cells also using WZ4002 as the anchor. Of the top scoring compounds for each cell line, the only one common to all three was the BCL-XL/BCL-2 inhibitor ABT263/navitoclax (Fig. 5a). Interestingly, prior laboratory studies have demonstrated that BCL-XL/BCL-2 inhibitors can enhance the apoptotic activity of targeted therapies that induce apoptosis by inducing BIM[17,32,33], presumably by decreasing the capacity for BCL-XL to neutralize BIM. The combination of WZ4002 and navitoclax induced a robust apoptotic response in low apoptosis T790M patient-derived cell lines (Fig. 5b) and in vitro generated T790M

resistant cell lines (Fig. 5c). In vivo, WZ4002 + navitoclax induced dramatic regression of MGH134 and PC9-GR3 xenograft tumors (Fig. 5d). Thus combining navitoclax with third generation EGFR inhibitors may be an effective strategy for T790M resistant cancers with decreased apoptotic response to EGFR inhibition. Indeed, the combination of AZD9291 and navitoclax will be tested in an upcoming clinical trial of EGFR NSCLC with acquired resistance to first line EGFR inhibitor therapy (NCT02520778).

Discussion

It is now well appreciated that significant genetic heterogeneity exists between cancer cell clones within a tumor[34]. While activating driver alterations such as the characteristic EGFR L858R mutation or exon 19 deletion are present in virtually every cell within an EGFR NSCLC tumor, the repertoire of accompanying mutations may vary[34,35]. While pre-existing intertumoral heterogeneity has been shown to influence treatment response and the development of acquired resistance to targeted therapy in some contexts[36], there has been surprisingly little direct clinical evidence supporting either emergence of pre-existing resistant clones or de novo evolution as the predominant mechanisms of acquired resistance in lung cancer. Several studies have reported the detection of low frequency T790M positive clones in pre-treatment clinical specimen[9,37], however doubts have been raised as to whether the majority of these may be simply sequencing artifacts related to tissue fixation[10].

Our results provide proof of principle that T790M clones not only emerge from selection of pre-existing clones but also can emerge from initially T790M-negative drug tolerant cells. Survival of drug tolerant cancer cells may be facilitated by cell autonomous features such as altered

epigenetic states[11,38] and feedback activation of alternate survival pathways[12] as well as external stimuli from the microenvironment[13,39]. While these mechanisms may be sufficient to prevent apoptosis and promote support survival of drug tolerant cells, they may not fully recapitulate the optimal oncogenic signaling provided by EGFR. Subsequent acquisition of T790M likely provides an additional fitness advantage in the presence of drug. Thus drug tolerant cells that are capable of surviving initial drug therapy may provide a reservoir of cells from which genetic mechanisms of acquired resistance can evolve. Such resistant clones may continue to share molecular features of the drug tolerant cells (Fig. 3e-f), leading to a diminished apoptotic response to subsequent therapies.

We believe that these findings have important clinical implications. These results provide a rationale for investigation of novel strategies for therapeutic targeting of drug tolerant cells before acquisition of genetic mechanisms of resistance in order to prevent or delay the evolution of acquired resistance and improve patient outcomes. We speculate that the majority of cancer cells that initially survive following therapy likely do not have *bona fide* resistant mechanisms (e.g., T790M), but more closely resemble a drug tolerant state. Since we now know that these drug tolerant cells can develop genetic mechanisms of resistance over time, we need to develop therapeutic approaches that kill this reservoir of drug tolerant cells that fail to undergo apoptosis. If successful, this should lead to more complete clinical remissions. Such treatment strategies will also need to integrate approaches that target the rare pre-existing *bona fide* resistant clones. We are hopeful that innovative approaches such as these will lead to markedly improved patient outcomes.

Figure Legends:

Figure 1. Variable sensitivity of T790M resistant PC9 cell lines to third generation EGFR inhibition.

a, PC9 parental cells were cultured in escalating concentrations of gefitinib as tolerated until fully resistant, which was defined as lack of inhibitory effect of drug on cell proliferation. PC9-GR2 resistant cells developed resistance more rapidly than PC9-GR3 cells.

b, PC9-GR3 cells have decreased apoptotic response to the third generation EGFR inhibitor WZ4002 compared to PC9-GR2 and parental cells. Cells were treated with 1 μM gefitinib (G), 1 μM WZ4002 (W) or vehicle (V) for 72 hours and apoptosis determined by annexin staining (data shown are mean and standard error of four independent experiments).

c, PC9-GR3 cells exhibit a net proliferative response to WZ4002 in vitro. Cells were treated with 1 μM gefitinib (GEF), 1μM WZ4002 (WZ) or vehicle (VEH) and cell proliferation was determined by CellTiter-Glo assay (mean and standard error of 4-5 independent experiments).

d, WZ4002 induces tumor regression of PC9-GR2 but not PC9-GR3 sub-cutaneous xenograft tumors. Mice bearing PC9-GR2 or PC9-GR3 subcutaneous xenograft tumors were treated with 50 mg/kg/day WZ4002. (PC9-GR2 - control (N=8), WZ (N=8); PC9-GR3 - control (N=8), WZ (N=8))

Figure 2. Early T790M acquired resistance results from selection of pre-existing T790M clones.

a, Rapid emergence of gefitinib resistant PC9 clones. PC9 parental cell pools were treated with 300 nM gefitinib for two weeks and cell viability was determined by CellTiter-Glo assay. 7% of

wells contained a rapidly proliferating resistant colony, while the remaining wells contained a small number of drug tolerant cells (inset). Each bar represents one well; data shown are combined from two independent experiments and are normalized to the mean viability of drug tolerant wells.

b, Early gefitinib resistant clones are sensitive to WZ4002. Upper panel, 50 early resistant clones were treated with gefitinib (GEF) or WZ4002 (WZ) for 72 hours and cell viability determined. Inset shows dose response of PC9 parental cells. Lower panel, cell viability of each early resistant T790M clone after treatment with 1 μM WZ4002 or gefitinib relative to vehicle control. Diagonal axis indicates equal sensitivity to both drugs (e.g. non-T790M), whereas sensitivity to WZ4002 but not gefitinib (lower right quadrant) indicates T790M. Parental cells are sensitive to both drugs and are shown for comparison.

c, Early gefitinib resistant cells are distinct from drug tolerant cells. PC9 cell pools (5,000 cells) were treated with 1 μM WZ4002 or 300 nM gefitinib + 500 nM NVP-AEW541 for two weeks and cell viability determined. WZ4002 suppressed emergence of early T790M resistant clones, whereas addition of AEW541 to gefitinib had no impact on emergence of early T790M clones despite elimination of drug tolerant cells.

d, ClonTracer barcoding technology demonstrates the pre-existence of early resistant gefitinib-resistant clones in the PC9 cell line, which were confirmed to harbor the T790M mutation (Supplementary Fig. 5b). The barcode distribution (fraction of each unique barcode in the total barcode reads) of one representative replicate each from CT-A barcoded cells treated with vehicle and gefitinib. The x-axes of the histograms are identical; each bar represents one unique barcode.

e, Percentage of enriched barcodes in each replicate that were also found in other replicates (1-5) for each independently barcoded experiment (CT-A,B,C). Colors denote the number of other replicates in which the barcodes were identified.

Figure 3. Late emerging T790M acquired resistance results from evolution of initially T790M-negative drug tolerant cells.

a, PC9 cell pools comprised of only drug tolerant cells were cultured in gefitinib until fully resistant. After 12 weeks of drug treatment, cells were partially resistant to both gefitinib and WZ4002 and negative for T790M by allele-specific PCR. After an additional 10-30 weeks, all were fully resistant to gefitinib and 5 of 16 had acquired T790M.

b, Late T790M resistant clones emerge from single cell-derived clone A after prolonged culturing in gefitinib.

c, Mathematical modeling of the acquisition of the T790M mutation within drug tolerant PC9 populations displaying the predicted frequency of PC9 cell pools (starting population 5000) developing a T790M mutation during 16 weeks of drug treatment as a function of mutational rate and cell division rate. Frequency values were calculated from the analytical solution and are represented as log10 of the percentage of wells predicted to develop T790M. Parameters that predict the experimentally observed 1.5% of wells acquiring T790M by 16 weeks are depicted by the solid (mean) and dotted (95% confidence interval) lines. The scale of the x-axis corresponds to a division rate of once very two weeks (low) to the rate of PC9 cells in the absence of drug (high).

d, Predicted frequency of acquiring T790M as a function of time calculated from the analytical solution of the model (black line is mean value, gray shaded area represents calculated standard

deviation). Parameters for drug tolerant cells: initial population size N_0=150, birth rate b=0.0162, death rate d=0.015, mutation rate μ=7.7x10^{-10}. The birth and death rates of T790M mutant cells are b_r=0.04 and d_r=0.0015, respectively[28].

e, Principal component analysis of global transcriptional profiles of PC9 parental, drug tolerant (selected in drug for 2 weeks; GT = gefitinib tolerant, WT = WZ4002 tolerant), early T790M PC9-GR2 and late T790M PC9-GR3 cells determined by RNA-Seq. Prior to harvesting RNA, cells were treated with vehicle or 1μM gefitinib (GEF) or WZ4002 (WZ) for 24 hours. PC9-GR3 cells cluster with drug tolerant cells.

f, Model for development of T790M acquired resistance from pre-existing T790M cells as well as evolution of initially T790M-negative drug tolerant cells.

Figure 4. Late evolving T790M acquired resistance is associated with decreased apoptotic sensitivity to third generation EGFR inhibition.

a, Late T790M PC9 resistant clones that emerged from parental and single cell-derived clones have decreased apoptotic response to WZ4002 compared to early resistant T790M clones that arose from pre-existing T790M cells. (Each dot represents an independent resistant clone, data shown are mean of 4-6 independent experiments. PAR = PC9 parental cells).

b, Gefitinib resistant MGH119 EGFR mutant NSCLC cells (GR1, GR2) that emerged after culturing in gefitinib for 5-6 months have decreased apoptotic response compared to parental cells (PAR) and MGH119-pTREX-T790M cells that were generated by introducing a Tet-inducible EGFR Del19/T790M construct. Expression of EGFR Del19/T790M was induced prior to the experiment by culturing in the presence of doxycycline. Cells were treated with 1 μM

gefitinib (G), WZ4002 (W) or vehicle (V). (Data shown are mean and standard error of 3-6 independent experiments.)

c, Patient-derived T790M EGFR mutant NSCLC cell lines have variable apoptotic response to WZ4002. (Data shown are mean and standard error of 4-7 independent experiments.)

d, Patient-derived cell lines with decreased apoptotic response have increased long term cell viability in the presence of WZ4002. Cells were treated with vehicle (open symbols) or 1 μM WZ4002 (closed symbols) and cell number determined by nuclear counting by high content imaging (mean and standard error of four replicates).

e, In vivo response of T790M cell line xenografts of WZ4002 mirrors in vitro apoptotic sensitivity. MGH134 and MGH141 sub-cutaneous xenograft tumors were treated with 50 mg/kg/day WZ4002 (closed squares), which suppressed growth of both xenograft tumor models compared with controls (open squares) but only induced regression of MGH141 tumors. (MGH134 - control (N=8), WZ (N=10); MGH141 - control (N=7), WZ (N=8))

f, Apoptotic sensitivity of patient-derived cell lines inversely correlates with duration of response of patient to first line EGFR inhibitor therapy. High apoptosis cell lines (MGH121, 164, 141); low apoptosis cell lines (MGH134, 157, 125, 138). Time to progression (TTP) was determined by time from initiation of therapy to first restaging scan showing definitive progression of disease. Statistical significance was calculated using the Mann-Whitney U test.

Figure 5. Navitoclax enhances apoptotic response of late T790M resistant cells with decreased sensitivity to third generation EGFR inhibition.

a, Top drug hits from a combination drug screen[14] that led to an enhancement of Emax when combined with WZ4002 in at least two of four T790M resistant cell lines screened. The response of MGH134 cells to ABT263 is shown as an example.

b, The combination of navitoclax (ABT263) and WZ4002 induces apoptosis in patient-derived T790M cell lines that have poor response to WZ4002 alone. (Data shown are mean and standard error of 4-7 independent experiments).

c, In vitro derived late T790M gefitinib resistant cell lines have increased apoptotic response to the combination of navitoclax and WZ4002 (Data shown are mean and standard error of 4-5 independent experiments).

d, Mice bearing MGH134 and PC9-GR3 subcutaneous xenograft tumors were treated with 100 mg/kg/day navitoclax and/or 50 mg/kg/day WZ4002. Robust tumor regression was observed only for the combination. (MGH134 N=8 control, 10 WZ, 8 ABT, 7 WZ+ABT; PC9-GR3 N=8 control, 8 WZ, 7 ABT, 7 WZ+ABT. Control and WZ data from Figures 1D and 3D are shown for comparison.)

Supplementary Figure Legends:

Supplementary Figure 1. Schematic depicting development of acquired resistance by either the emergence of a pre-existing resistant clone (e.g. T790M) versus evolution of a drug tolerant intermediate that acquires the genetic resistance mechanism during the course of drug treatment.

Supplementary Figure 2. WZ4002 inhibits EGFR phosphorylation and downstream MEK and PI3K signaling in PC9, GR2 and GR3 cells, but fails to up-regulate BIM and induce mitochondrial depolarization in PC9-GR3 cells. a, Cells were treated with 1 μM gefitinib (G), WZ4002 (W) or vehicle (V) for 24 hours and lysates harvested for western blotting. **b,** Transcriptional outputs of MEK/ERK (DUSP6, SPRY4) and PI3K/AKT signaling (HER3, DAPK1) are modulated equally by WZ4002 in PC9, GR2 and GR3 cells. Cell were treated with 1 μM WZ4002 or vehicle for 24 hours. Gene transcript levels were determined by quantitative RT-PCR and normalized to ACTIN. Values shown are fold difference in transcript level after WZ4002 treatment relative to vehicle control. **c,** Cells were treated with 1 μM WZ4002 for 18 hours and cell cycle populations were determined by propidium iodide staining. There was no statistical difference between the % increase in cells in G1 or % decrease in cells in S phase after WZ4002 treatment between any of the three cell lines.
d, Cells were treated with 1 μM gefitinib (G), WZ4002 (W) or vehicle (V) in the presence of the pan-caspase inhibitor 10 μM QVD-Oph in triplicate. After 48 hours, cells were harvested and stained with JC-1 (Life Technologies) and analyzed by flow cytometry. **e,** Cells were treated with 1 μM WZ4002 for 24 hours in duplicate and RNA harvested for RNA-Seq analysis. Values

shown are log2 fold change after WZ treatment. **f,** BIM mRNA transcript levels were quantified by quantitative RT-PCR following treatment with 1 μM WZ4002 for 24 hours and normalized to GAPDH. Values shown are mean and standard error of three independent experiments. **g,** Cells were treated with 1 μM gefitinib (G), WZ4002 (W) or vehicle (V) and harvested for western blotting. Band intensities were quantitated by densitometric analysis and normalized to vehicle control; values shown are mean and standard error of four independent experiments. **h,** Induction of apoptosis is necessary for cytotoxic response of PC9-GR2 cells to WZ4002 in vitro. Cells were treated with vehicle or 1 μM WZ4002 in the presence or absence of 20 μM QVD-Oph (pan-caspase inhibitor). Apoptosis was determined by annexin staining after 72 hours. Cell proliferation was determined by CellTiter-Glo assay. Blocking the apoptotic response in PC9-GR2 cells resulted in cytostatic response similar to PC9-GR3 cells (see Fig. 1c).

Supplementary Figure 3. Inhibition of EGFR and ERK phosphorylation after WZ4002 treatment in xenograft tumors. Mice were treated with 50 mg/kg/day WZ4002 daily and tumors were harvested 3 hours after the day 3 dose for western blot analysis. Phosphorylated EGFR and phosphorylated ERK1/2 band intensities were quantified by densitometric analysis, and each data point is the relative phospho-protein abundance from an individual mouse. Asterisks indicate that statistically significant decreases in EGFR and ERK phosphorylation were observed after drug treatment for all models. There were no significant differences in phosphorylation levels in drug treated tumors between a, GR2 versus GR3 and b, MGH141 versus MGH134 models.

Supplementary Figure 4. Characterization of T790M alleles in gefitinib resistant PC9 cells. **a,** T790M allele specific quantitative PCR performed on genomic DNA isolated from 50 early gefitinib resistant clones revealed that all harbor the T790M mutation. Values shown are the difference in Cp values between the T790M specific probe and deletion 19 control. **b,** EGFR is amplified in PC9 cells. Relative EGFR amplification assessed by quantitative PCR on genomic DNA. Copy number relative to LINE1 and chromosome 7 was calculated after normalization to MGH1075 (stromal fibroblast DNA) diploid control. **c,** T790M allelic abundance in PC9-GR2 and PC9-GR3 cells as determined by droplet digital PCR and next generation sequencing corresponds to one mutant allele per 8-10 total EGFR alleles. d, Single cell clones of PC9-GR2 and PC9-GR3 lines were established and assayed for the presence of T790M. All clones examined were T790M positive, ruling out the alternative possibility that the observed T790M fractional abundance (ddPCR) and VAF (NGS) is due to a mixed population of T790M-positive and negative cells.

Supplementary Figure 5. ClonTracer barcode analysis of gefitinib treated PC9 cells. a, Schematic of ClonTracer (CT) experimental setup. Three independent barcoded PC9 populations were generated (CT-A, CT-B, CT-C) and treated in identical fashion, **b,** T790M allele specific PCR demonstrates that gefitinib treated PC9 populations are enriched for early resistant T790M clones. **c,** Barcode complexity of vehicle treated (pre-treatment) and gefitinib selected PC9 populations as determined by next generation sequencing of barcodes. To accomodate the barcode complexity observed in vehicle treated groups, top 95% of the total cell population was used for estimating the number of unique barcodes. **d,** Heatmap depicting barcode abundance in pre-treatment and gefitinib treated PC9 populations. Note that replicates of the same transduced

pool exhibit substantial overlap of enriched barcodes, whereas there is negligible overlap of barcodes between each of the three independent pools.

Supplementary Figure 6. Emergence of T790M resistant clones from drug tolerant cells. **a,** Intermediate resistant PC9 cells expanded from drug tolerant cells (after 12 weeks gefitinib treatment) are negative for T790M by allele specific qPCR. **b,** A subset of late (fully) gefitinib resistant PC9 cells derived from drug tolerant cells acquire T790M. Asterisks denote WZ4002 sensitivity of T790M positive late resistant cells. **c,** Fractional abundance of T790M cells can be determined by T790M allele specific qPCR. Intermediate freeze-downs of PC9-GR3 cells during the development of gefitinib resistance were assayed for the presence of T790M. Red line shows gefitinib dose tolerated as a function of time and is replotted from Fig. 1a. Gray bars show fraction of T790M cells in population. Inset shows calibration of standard curve. No T790M was detected prior to 5 months (threshold for detection 1.5%), where as 6% of population was T790M positive at 5.5 months. d. Fraction of T790M cells (red bar) at intermediate time points for selected late resistant T790M clones. PC9-GR3 is shown for comparison. The dotted line depicting an exponential growth curve fit to the data is shown for illustrative purposes.

Supplementary Figure 7. Assessment of drivere gene amplification in late non-T790M resistant clones. Assessment of MET, KRAS, EGFR, HER2, NRAS and BRAF amplification by quantitative PCR on genomic DNA from late gefitinib resistant PC9 clones. Copy number relative to LINE1 (MET, KRAS, EGFR, HER2, NRAS and BRAF), chromosome 12 (KRAS) or chromosome 7 (MET, EGFR, BRAF) was calculated after normalization to MGH1075 (stromal

fibroblast DNA) diploid control. HCC827-GR6 is MET amplified positive control, H358 is KRAS amplified positive control.

Supplementary Figure 8. T790M can emerge from drug tolerant clones. a, No early T790M resistant clones were observed after treating ten independent PC9 single cell sub-clones (5,000 cells/well) with gefitinib for two weeks. **e,** A subset of gefitinib resistant clones emerging from PC9 single cell sub-clone A develop T790M. **c,** Introduction of pre-existing T790M cells into single cell clone populations recapitulates emergence of early resistant clones. An early T790M resistant clone (see Fig. 2b) was labeled with RFP to generate PC9-T790M-RFP cells, which were spiked into a combined background of unlabeled single cell-derived clonal lines A-D at a frequency of 1:10,000. Cells were treated gefitinib and cell viability was measured weekly with the RealTime-Glo assay. **d,** The number of resistant wells that were newly detected at each time interval for two independent experiments. **b,** A cumulative density function modeling the emergence of PC9-T790M-RFP clones indicates that 72.6% of emerging pre-existing T790M clones are detectable 2 weeks after starting gefitinib treatment. We observed that 4 out of 4 single cell clone lines yielded late T790M resistant clones. The probability that these late T790M clones emerged from undetected pre-existing T790M cells is $0.274^4 = 0.006$.

Supplementary Figure 9. Estimating growth rate of PC9 drug tolerant cells in the presence of gefitinib. a, PC9 pools were treated with 300 nM gefitinib and cell number tracked over time using RealTime-Glo assay. The population sizes between weeks 5-10 were used to fit growth parameters for mathematical modeling of evolution of T790M from drug tolerant cells (see Fig. 3c-d). **b,** Comparison between analytical solution (black squares) and the Monte Carlo

simulation (red circles) shows very close correlation between predicted frequency of acquiring the T790M mutation in drug tolerant cells. The inset compares the correlation between the simulation (10,000 runs) and the analytical solution with the calculated theoretical standard error range. **c,** 484 pools of 5000 PC9 cells representing 8 different single cell clonal lines were treated with 300 nM gefitinib. By 16 weeks, 203 pools with developing resistance had expanded to sufficient numbers to perform T790M genotyping. 3/200 were found to be T790M positive.

Supplementary Figure 10. The MGH119 cell line does not harbor pre-existing T790M cells. **a,** No early resistant colonies emerge from MGH119 cells upon gefitinib treatment. MGH119 cell pools (5,000/well) were treated with 300 nM gefitinib for three weeks and cell viability determined with CellTiter-Glo assay. **b,** Modeling emergence of pre-existing MGH119 T790M clones. MGH119-GR1 cells were labeled with RFP and introduced at low frequency into a background of unlabeled MGH119 parental cells. Cells (120 wells, 5,000 cells/well) were treated with 300 nM gefitinib and emerging resistant colonies were monitored by RealTime-Glo assay and RFP fluorescence. Note that all emerging resistant colonies derive from the introduced RFP-labeled pre-existing T790M cells. Right panel shows cell viability for all wells (each bar represents one well) at 10 weeks.

Supplementary Figure 11. RNA-Seq analysis of PC9 cell populations. a, Proposed evolutionary relationship of samples analyzed by RNA-Seq. **b,** Heatmap of top and bottom 600 genes contributing most strongly to variance of PC2 demonstrates clustering of PC9-GR3/drug tolerant versus PC9-GR2/parental cells. **c,** Gene set enrichment analysis (GSEA) was performed comparing differentially expressed genes between PC9-GR3/drug tolerant and PC9-

GR2/parental cell groups to Hallmark and Oncogenic Signature gene sets in the Molecular Signatures Database (MSigDB). Six gene sets were significantly enriched with a FDR q-value less than 0.01. The most significantly enriched gene set correlating with genes upregulated in PC9-GR3/drug tolerant was epithelial-to-mesenchymal transition. (EMT-related gene sets are highlighted in yellow.) **d,** Significant enrichment of genes associated with TGF-β induced EMT in lung cancer cells (GSE17708) was also observed in PC9-GR3/drug tolerant cells.

Supplementary Figure 12. Drug tolerant cells are characterized by loss of apoptotic response despite inhibition of EGFR signaling. a, Gefitinib tolerant PC9 cells have decreased apoptotic response to EGFR inhibition. PC9 parental cells were treated with gefitinib for two weeks and apoptotic response to 1 μM gefitinib or WZ4002 was determined (PAR = parental cells, GEF DT = gefitinib tolerant cells). **b,** Drug tolerant cells maintain residual pAKT and pERK signaling in the presence of gefitinib and have impaired upregulation of BIM.

Supplementary Figure 13. Acquisition of T790M by drug tolerant cells leads to emergence of T790M clones with reduced apoptotic sensitivity to WZ4002. a, To model evolution of T790M from drug tolerant cells, PC9 cells were treated with 300 nM gefitinib for 4 weeks to generate T790M-negative drug tolerant cells. Pools of 1000 drug tolerant cells in 96-well plate format were infected with lenti pTREX-DEL19/T790M at a low titer to infect approximately 1 cell every other well. Cells were treated with doxycycline (DOX) to induce expression of T790M and then cultured in the presence of gefitinib. Cell number was assayed weekly using RealTime-Glo. After approximately 3 weeks, pTREX-DEL19/T790M resistant colonies were detected above background drug tolerant cells. Red lines indicate wells with emerging pTREX-

DEL19/T790M clones, black lines indicate wells with only drug tolerant cells. After 30 days, all cells were treated with puromycin to distinguish which drug tolerant clones contained the pTREX-DEL19/T790M transgene (designated PC9 DT-DEL19/T790M) and to eliminate uninfected drug tolerant cells. Nine out of ten clones tested had reduced apoptotic sensitivity to WZ4002 compared to PC9 parental cells infected with lenti pTREX-DEL19/T790M (and pTREX-DEL19 and pTREX-GFP controls), which represent pre-existing T790M cells (G = Gefitinib, W= WZ4002; data are expressed as % apoptosis above vehicle control). **b,** Western blot confirmation of expression of T790M EGFR in three pTREX-DEL19/T790M drug tolerant clones. Cells were treated with 1 μM geftinib or WZ4002 for 24 hours. **c,** Western blot confirmation of expression of T790M EGFR in MGH119-pTREX- T790M cells (see Fig. 4b)

Supplementary Figure 14. Rationale for re-analyzing patient-derived cell line combination drug screen data. Loss of apoptotic response in PC9-GR3 cells manifests more prominently as a change in Emax rather than shift in GI50.

Methods

Cell lines

The EGFR mutant NSCLC PC9 cell line (EGFR exon 19 del E746_A750, EGFR amplified) was obtained from the MGH Center for Molecular Therapeutics. The identity of PC9 parental, GR2 and GR3 cell lines were verified by STR analysis (Bio-synthesis, Inc.) at the time that these studies were performed. EGFR mutant NSCLC patient-derived cell lines were established in our laboratory from core biopsy or pleural effusion samples as previously described[14,40]. The MGH1075 stromal fibroblast line was established in our laboratory from a surgical resection specimen of an early stage primary lung adenocarcinoma. All patients signed informed consent for an IRB-approved protocol giving permission for research to be performed on their samples. The HCC827-GR6 line (Exon 19 deletion, MET amplified) was previously described[6]. H358 cells were obtained from the Center for Molecular Therapeutics at MGH. PC9-T790M-RFP and MGH119-GR1-RFP cells were generated by infecting the PC9 Early T-1 clone and MGH119-GR1 cells, respectively, with Cignal Lenti RFP (Qiagen) lentivirus followed by puromycin selection. All cell lines were maintained in RPMI supplemented with 10% FBS, except MGH125 and MGH138 cells which were maintained in ACL4 with 10% FBS and TCM with 10% FBS, respectively. All experiments were performed in RPMI with 10% FBS. All cells were routinely tested and verified to be free of mycoplasma contamination.

Antibodies and reagents

For western blotting, the following antibodies were used: phospho-EGFR Y1068 (Abcam); EGFR, pERK1/2 T202/204, ERK1/2, p-AKT S473, Actin (Cell Signaling); AKT1/2/3 (Santa

Cruz). For cell culture studies, gefitinib, WZ4002, NVP-AEW541, ABT-263 (all from Selleck), were dissolved in DMSO to a final concentration of 10 mmol/l and stored at –20°C. Unless otherwise specified, 1 μM concentration was used for in vitro cell culture experiments.

In vitro generation of gefitinib resistant cell lines

Gefitinib resistant PC9-GR2, PC9-GR3 and MGH119-GR1 cells were established by culturing parental cells in escalating concentrations of gefitinib (10 nM – 1 μM) as tolerated as previously described [14]. MGH119-GR2 cells were established by culturing parental cells in full dose gefitinib (1 μM). Early, drug tolerant, late PC9 resistant clones were established by culturing in 300 nM gefitinib until resistant, at which point they were maintained in 1 μM gefitinib. During generation of resistance, media and drug were replaced twice per week.

Generation of PC9 single cell sub-clones

PC9 parental cells were seeded into 96-well plates at a density of 0.5 cells/well. After 2 weeks, approximately 25-40% of wells (50-80% of theoretical yield) contained colonies of about 10,000 cells. A minority of wells contained two colonies, which were easily distinguishable. Wells containing only single colonies were expanded an additional 6-10 doublings for use in experiments.

PI/Annexin apoptosis assay

Cells were seeded at low density 24 hours prior to drug addition. 72 hours after adding drugs, floating and adherent cells were collected and stained with propidium iodide and Cy5-Annexin V

(BD Biosciences) and analyzed by flow cytometry. The annexin-positive apoptotic cell fraction was analyzed using FloJo software.

CellTiter-Glo proliferation

For dose response assays, cell lines were seeded into 96-well plates 24 hours before addition of drug. Cell proliferation was determined by CellTiter-Glo assay (Promega) 72 hours after adding drug using standard protocols. For time course experiments, multiple plates were seeded and drugged in identical fashion and at indicated time points plates were frozen at -80^{o}C; all plates in an experiment were developed with CellTiter-Glo simultaneously. For early resistant/drug tolerant cell experiments, CellTiter-Glo was performed at indicated times on cells in situ.

RealTime-Glo viability assay

Cell viability was assayed in situ once weekly starting the day after seeding using the RealTime-Glo assay (Promega) according to the manufacturers protocol. Briefly, MT Cell Viability Substrate and NanoLuc Enzyme were diluted 1:500 in media and 25 μl was added to each well (1/5 total final volume). Cells were incubated for 1 hour at 37^{o}C and luminescence measured. For experiments including RFP-labeled cells, RFP fluorescence was measured using Ex 553 nm/Em 574 nm. We did not observe any effect of the presence of RFP on RealTime-Glo luminescence or vice versa. Fresh media containing gefitinib was replaced immediately after each assay.

Long term viability assay

Long term viability assays were completed by plating 1,000-4,000 cells/well in replicate 96-well plates. Cells were treated in quadruplicate 2x/week and fixed at days 0, 3, 7, 14, 21, 28 and 35 with a mixture of formaldehyde (1.0%), PBST (0.04%), and Hoecsht dye (1ug/ml). Stained nuclei were imaged and then counted using a Molecular Devices ImageXpress Micro high content imager and MetaXpress software.

Cell cycle Analysis

Cells were seeded 24 hours prior to experiment to give a confluency of 30-50%. Drugs were added for 24 hours and cells harvested, stained with propidium iodide and analyzed by flow cytometry. Cell cycle sub-populations were calculated using the FloJo software cell cycle module.

JC-1 mitochondrial depolarization assay

Cells were treated with EGFR inhibitor in the presence of 10 μM QVD-Oph to prevent subsequent apoptosis. 48 hours after drug treatment, cells were harvested and stained with JC-1 (Life Technologies) according to the manufacturers recommendations. 10 μM CCCP was used as a positive control. Cells were analyzed by flow cytometry using excitation/emission filters for PE and FITC. Mitochondrial depolarization is indicated by a decrease in the red/green fluorescence intensity ratio.

Quantitative RT-PCR assay for gene expression

Cells were seeded 24 hours prior to give a confluency of 50%. Cells were treated with drugs for 24 hours and RNA was extracted using the RNeasy Kit (Qiagen). cDNA was prepared from 500

ng total RNA with the First Strand Synthesis Kit (Invitrogen) using oligo-dT primers. Quantitative PCR was performed using FastStart Sybr Green (Roche) on a Lightcycler 480. mRNA expression relative to ACTIN was calculated using the Delta-Delta threshold cycle method. Primers used: DUSP6 F 5'-CGACTGGAACGAGAATACGG-3', R 5'-TTGGAACTTACTGAAGCCACCT-3'; SPRY4 F 5'- CCCCGGCTTCAGGATTTA-3', R 5'-CTGCAAACCGCTCAATACAG-3'; HER3 F 5'-CTGATCACCGGCCTCAAT-3', R 5'-GGAAGACATTGAGCTTCTCTGG-3'; DAPK1 F 5'-CCCTTGTCCCAGTTGAAGAA-3', R 5'-CCGGTCGAGGAACATTCA-3'; BIM F 5'- GATCCTTCCAGTGGGTATTTCTCTT-3', R 5'-ACTGAGATAGTGGTTGAAGGCCTGG-3; Actin F 5'-CTGTGCTATCCCTGTACGCCTC-3', R 5'-CATGATGGAGTTGAAGGTAGTTTCGT-3'; GAPDH F 5'-AACAGCGACACCCATCCTC-3', R 5'-CATACCAGGAAATGAGCTTGACAA-3.

T790M quantitative PCR assay

The T790M mutation was detected using allele specific primers (F) 5'-ACCATGCGAAGCCACACTGACG-3' and (R) 5'-AGCCGAAGGGCATGAGCTGGA-3' in conjunction with an EGFR exon 20 Taqman probe 5'-ATCACGTAGGCTTCCTGGAG-3'. A commercially available EGFR exon 19 deletion Taqman assay was used as a reference (Hs00000228_mu, Life Technologies). Quantitative PCR was performed on genomic DNA using either FastStart PCR Master or Lightcycler 480 Probes Master kits (Roche) on a Lightcycler 480. For screening assays, ΔCp(T790M-DEL19) < 8 was considered positive and ΔCp > 10 was considered negative (Probes Master), or ΔCp < 14 positive/ΔCp > 16 negative (FastStart).

EGFR T790M droplet digital PCR analysis

Isolated gDNA was amplified using ddPCR™ Supermix for Probes (Bio-Rad) with EGFR p.T790M (PrimePCR™ ddPCR™ Mutation Assay, Bio-Rad) for point mutation detection. ddPCR was performed according to manufacturer's protocol and the results reported as percentage or fractional abundance of mutant DNA alleles to total (mutant plus wild type) DNA alleles. 8 to 10 µl of DNA template was added to 10 µl of ddPCR™ Supermix for Probes (Bio-Rad) and 2 µl of the primer/probe mixture. Droplets were generated using Auto-DG where the reaction mix was added together with Droplet Generation Oil for Probes (Bio-Rad). Droplets were then transferred to a 96 well plate (Eppendorf) and then thermal cycled with the following conditions: 5 minutes at 95°C, 40 cycles of 94°C for 30s, 55°C for 1 minute followed by 98°C for 10 minutes (Ramp Rate 2°C/sec). Droplets were analyzed with the QX200™ Droplet Reader (Bio-Rad) for fluorescent measurement of FAM and HEX probes. Gating was performed based on positive and negative controls, and mutant populations were identified. The ddPCR data were analyzed with QuantaSoft analysis software (Bio-Rad) to obtain Fractional Abundance of the mutant DNA alleles in the wild-type/normal background. Fractional Abundance is calculated as follows: F.A. % = (Nmut/(Nmut+Nwt))*100), where Nmut is number of mutant events and Nwt is number of WT events per reaction. ddPCR analysis of normal control (from cell lines) and no DNA template controls were always included. Samples with too low positive events were repeated at least twice in independent experiments to validate the obtained results.

Clinical cancer genotyping analysis

DNA was extracted from late non-T790M gefitinib resistant PC9 clones using the DNeasy kit (Qiagen). Genotyping was performed using the MGH NGS platform which utilizes a multiplex polymerase chain reaction (PCR) technology called Anchored Multiplex PCR (AMP) for single

nucleotide variant (SNV) and insertion/deletion (indel) detection in genomic DNA using next generation sequencing (NGS). Genomic DNA was sheared with the Covaris M220 instrument, followed by end-repair, adenylation, and ligation with an adapter. A sequencing library targeting hotspots and exons in 39 genes was generated using two hemi-nested PCR reactions. Illumina MiSeq 2 x 151 base paired-end sequencing results were aligned to the hg19 human genome reference using BWA-MEM. MuTect and a laboratory-developed insertion/deletion analysis algorithm were used for SNV and indel variant detection, respectively. This assay has been validated to detect SNV and indel variants at 5% allelic frequency or higher in target regions with sufficient read coverage. Variants are reported with Human Genome Variation Society (HGVS) protein and DNA nomenclature, followed by the referenced Ensembl transcript ID. The gene targets covered by this assay are as follows (exons): AKT1 (3), ALK (22, 23, 25), APC (16), BRAF (11, 15), CDH1 (1, 2, 3, 4, 5, 6, 7, 8, 9, 10, 11,12, 13, 14, 15, 16), CDKN2A (1, 2, 3), CTNNB1 (3), DDR2 (12, 13, 14, 15, 16, 17, 18), EGFR (7, 15, 18, 19, 20, 21), ERBB2 (10, 20), ESR1 (8), FBXW7 (1, 2, 3, 4, 5, 6, 7, 8, 9, 10, 11), FGFR1 (4, 8, 15, 17), FGFR2 (7, 9, 12,14), FGFR3 (7, 8, 9, 14, 16), FOXL2 (1), GNA11 (5), GNAQ (4, 5), GNAS (6, 7, 8, 9), HRAS (2, 3), IDH1 (3, 4), IDH2 (4), KIT (8, 9, 11, 17), KRAS (2, 3, 4, 5), MAP2K1 (2, 3), MET (14, 16, 19, 21), NOTCH (25, 26, 34), NRAS (2, 3, 4, 5), PDGFRA (12, 14, 18, 23), PIK3CA (2, 5, 8, 10, 21), PIK3R1 (1, 2, 3, 4, 5, 6, 7, 8, 9, 10), PTEN (1, 2, 3, 4, 5, 6, 7, 8, 9), RET (11, 16), ROS1 (38), SMAD4 (2, 3, 4, 5, 6, 7, 8, 9, 10, 11, 12), SMO (9), STK11 (1, 2, 3, 4, 5, 6, 7, 8, 9), TP53 (1, 2, 3, 4, 5, 6, 7, 8, 9, 10, 11), and VHL (1, 2, 3).

Gene amplification quantitative PCR assay

Quantitative PCR was performed on genomic DNA using FastStart Sybr Green (Roche) on a

Lightcycler 480. Primers for KRAS, MET, Chromosome 12 control, Chromosome 7 control were previously described[41]. EGFR, BRAF and NRAS primers were adapted from Dias-Santagata et al[42]: EGFR F 5'- CCTCCTTCTGCATGGTATTC-3', R 5'-GCAGCATGTCAAGATCACAG-3'; BRAF F 5'- TGCTTGCTCTGATAGGAAAATG-3', R 5'-CTGATGGGACCCACTCCAT-3'; NRAS F 5'- CAACAGGTTCTTGCTGGTGT-3', R 5'-GAGAGACAGGATCAGGTCAGC-3'. LINE1 primers: F 5'-AAAGCCGCTCAACTACATGG -3', R 5'-TGCTTTGAATGCGTCCCAGAG -3'). ΔCp between gene-control (KRAS - Chr.12, LINE1; MET, EGFR, BRAF - Chr. 7, LINE1; HER2, NRAS - LINE1) were calculated and normalized to MGH1075 diploid fibroblast control. HCC827-GR6 were used as a MET amplification control [6] and H358 cells were used as KRAS amplification control.

Generation of Tet-inducible EGFR pTREX cell lines

Exon 19 del and Exon 19 del/T790M plasmids were purchased from Addgene (32062, 32072). EGFR sequences were PCR amplified with the F 5'-CACCATGCGACCCTCCGGGACG-3' and R 5'-TCATGCTCCAATAAATTCACTG-3' primers and ligated into the pENTR/D-TOPO vector using the pENTR Directional TOPO Cloning Kits (Invitrogen). The sequence was then introduced into the pTREX vector (kindly provided by Novartis) using Gateway LR Clonase Enzyme (Invitrogen). The pTREX-DEL19 and pTREX-DEL/T790M vectors were subsequently verified by DNA sequencing. Lentivirus was produced using standard procedures[43]. PC9 and MGH119 cells were infected with lentivirus followed by puromycin selection. Cells were cultured in the presence of 10 ng/ml doxycycline to induce expression of EGFR construct. For

infection of PC9 drug tolerant single cells, cells were infected with a lentiviral titer that yielded a single puromycin resistant colony in ~50% of wells.

Mouse xenograft studies

All mouse studies were conducted through Institutional Animal Care and Use Committee–approved animal protocols in accordance with institutional guidelines. For xenograft studies, cell line suspensions were prepared in 1:10 matrigel and $5x10^6$ cells were injected subcutaneously into the flanks of female athymic nude (Nu/Nu) mice (6-8 weeks). Visible tumors developed in approximately 2-4 weeks. Tumors were measured with electronic calipers and the tumor volume was calculated according to the formula $V = 0.52 \times L \times W^2$. Mice with established tumors were randomized to drug treatment groups using covariate-adaptive randomization to minimize differences in baseline tumor volumes: WZ4002 50 mg/kg (10% 1-methyl-2-pyrolidone, 90% PEG300), ABT-263 100 mg/kg (30% PEG400/60% Phosal 50 PG/10% ethanol), or combinations. Drug treatments were administered by oral gavage and tumor volume measured twice weekly as above. For pharmacodynamic studies, mice were sacrificed and tumors removed 3 hours after drug administration on day 3. Tumors were snap frozen and lysates prepared for western blotting. Investigators performing tumor measurements were not blinded to treatment group. Sample size (minimum N=7 per treatment group) was chosen to verify satisfactory inter-animal reproducibility.

ClonTracer barcode library

Construction of the ClonTracer barcode library and generation of lentiviral particles was previously described[8]. Pools of 10 million PC9 cells were barcoded by lentiviral infection at a

MOI of 0.1-0.2 and infected cells were selected with puromycin. Infected cell populations were expanded in culture for the minimal time period to obtain a sufficient number of cells to set up replicate experiments. 20 million cells (~10x barcode representation) were seeded in multiple replicate plates and treated with vehicle or 300 nM gefitinib (5 replicates). Vehicle treated cells reached confluency within 3 days and the entire pool was pelleted and snap frozen. Gefitinib treated plates became confluent from emergence of early resistant clones and were harvested after 3 weeks. Cell counts were approximately 20 million cells per replicate plate. Genomic DNA was extracted from the frozen cell populations with a QIAamp DNA Blood Maxi Kit (Qiagen). We used PCR to amplify the barcode sequence for NGS and introduce Illumina adaptors and index sequences[8]. PCR primer sequence information can be found at https://www.addgene.org/pooled-library/clontracer/. The sampling of sufficient template coverage was ensured by parallel PCR reactions.

PCR-amplified products were sequenced on an Illumina HiSeq2500 sequencer in Rapid Mode using the 50 Cycle TruSeq Rapid v2 SBS Kit, TruSeq Rapid SR v2 Cluster Kit, and HiSeq Rapid SR v2 Flow Cell (Illumina) as previously described[8].. Barcode-composition analysis was carried out as previously described[8]. A barcode was called significant if it was seen at more than 0.01% of the total population in the drug treated samples (10 times the fraction of the most enriched barcode in the vehicle treated replicates).

Cumulative density function modeling of emergence of T790M clones

Using the cumulative number (N) of RFP+ clones detected at each time point, a best fit model (without being highly sensitive to local noise) was calculated with the Matlab Curve Fitting Tool with fittype exp2, representing a model of the form a*exp(b*x) + c*exp(d*x). The 95%

confidence bounds for the coefficients of equation 1 were: a = 53.56 (47.19, 59.93), b = 0.0002647 (-0.001714, 0.002243), c = -53.58 (-60.17, -47), d = -0.09483 (-0.1178, -0.07186). The equation:

$$ft = 53.56\ e^{.0002647t} - 53.58\ e^{-0.09483t}$$
$$r^2 = 0.9981$$

was normalized by the value f(70)=54.492, transforming it into a cumulative density function with values ranging from [0,1]:

$$\frac{53.56\ e^{.0002647t} - 53.58\ e^{-0.09483t}}{54.492}$$

The value of the CDF at t(14 days) = 0.7259, representing the probability that a pre-existing T790M clone would emerge within 14 days. The probability that a pre-existing T790M would not emerge within 14 days is 1-0.7259= 0.2741. The probability of this occurring in 4 independent trials= 0.2741^4= 0.0056.

Estimation of frequency of pre-existing T790M clones in parental PC9 cell stock

After 2 weeks of drug exposure, 90 of 1260 wells were detected to contain resistant T790M colonies. Based on the above modeling of emergence of pre-existing RFP-labeled T790M clones, this represents approximately 72% of pre-existing T790M cells. Thus the theoretical frequency of pre-existing T790M can be estimated:

$$\frac{(90 \text{ colonies}/0.7259)}{1260 \text{ wells} \times 5000 \text{ cells/well})} = 0.00001968 \approx 1{:}50000$$

From experiments generating PC9 single cell clones, the efficiency of single PC9 cells to establish progeny is between 50-80%, thus the frequency of T790M cells in our parental PC9 line is approximately 1:25000 – 1:50000.

Mathematical modeling of evolution of T790M from drug tolerant cells

To model de novo acquisition of the T790M mutation during drug treatment, we assumed a branching process[27] comprised of N_0 drug tolerant cells that divide at a rate b, die at rate d, and upon birth, mutate at a rate μ. Acquisition of T790M mutations yields resistant cells divide at a rate of b_r and die at a rate d_r. The range of values of the birth and death rates of drug tolerant cells were based on single cell parameters reported by Tyson et al.[28] and fit to population growth rates determined by tracking the growth of pools of PC9 drug tolerant during weeks 5-11 of gefitinib treatment (Supplementary Fig. 9a). The average estimated growth rate determined by fitting the growth curves to an exponential function from the week with the smallest population, which was usually week 6 until week 11, and taking the average was b-d =0.0015±[0.0012]/h. Using the inferred growth rate we back extrapolated the initial population size of the drug tolerant cells to be on average N_0 = 150±23. Once a cell acquired the T790M mutation, the birth and death rate of the resulting T790M resistant cells were assumed to have similar rates as PC9 parental cells in the absence of drug (Tyson et al[28] as well as our own unpublished data). Currently there are is no agreement on the average mutation per SNV per cell division, and estimation ranges from10^{-11} up to 10^{-7} for non-hypermutator cells[44,45]. More recent estimates range from 10^{-10} to 10^{-8} [46], with a slight tendency towards lower values. Of note, the EGFR T790M mutation is a change of ACG to ATG generated by spontaneous deamination of 5-methylcytosine to uracil, which occurs at 18 times greater than the average rate[47]; furthermore the EGFR gene has a rate that is about twice the average rate[46] across the genome (MutSigCV[48] estimation output). Gene amplification can increase the allelic pool in which a mutation can arise, and PC9 cells have EGFR gene amplification (10 copies per cell, see Supplementary Fig.

4b) with a single T790M mutation being sufficient to confer drug resistance. Thus effectively the rate of getting a T790M mutation is about 360 times more likely than an average SNV.

We modeled the process with a Monte Carlo simulation in order to estimate the fraction of drug tolerant pools predicted to acquire T790M by16 weeks after beginning drug treatment. Conversely, we simulated the fraction of drug tolerant pools predicted to acquire T790M as a function of time using fixed parameters. Additionally we derived an analytical approximation to the model

$$R = 1 - (1-\mu)^{\frac{N_0 e^{(b-d)T}}{b-d} b} \sim \frac{N_0 e^{(b-d)T}}{b-d} b\mu$$

where *R* represent the fraction of PC9 drug tolerant pools that acquire a T790M mutation as a function of time (*T*). In Supplementary Fig. 9, we compare the results of the analytical solution (black line) to the Monte Carlo simulations (red dots) based on 10,000 runs per set of values. One can see that they match very well. The logic behind the solution, is to estimate the number of birth events during from day 0 to the end of the experiment which is

$$\frac{N_0 e^{(b-d)T}}{b-d} b$$

and calculating the probability of having at least one T790M mutation. One should have in mind that the mutation rate in the equation is not the average mutation per SNV per cell division, rather 360 times larger, as explained above. It is possible that prior models may not have taken this into account, which may explain the differences in the assumed baseline mutational rates between our model and prior models (e.g. 10^{-8}-10^{-7})[27].

RNA-Seq analysis

Total RNA was isolated using the RNeasy Mini Kit (Qiagen). RNA-Seq libraries were constructed from polyA-selected RNA using NEBNext Ultra Directional RNA library prep kit for Illumina (New England Biolabs) and sequenced on Illumina HiSeq2500 instrument, resulting in approximately 34 million reads per sample on average. STAR aligner[49] was used to map sequencing reads to transcripts in human hg19 reference genome. Read counts for individual transcripts were produced with HTSeq-count[50], followed by the estimation of expression values and detection of differentially expressed transcripts using EdgeR[51]. Principle component analysis (PCA) was performed on the union of differentially expressed transcripts in all samples. We used the package for gene-set enrichment analysis (GSEA)[52,53] to analyze the enrichment of functional gene groups among differentially expressed transcripts. Normalized enrichment score (NES) and enrichment plots were calculated based on gene lists ranked by expression ratio between early (PC9 parental and PC9-GR2) and late (PC9-GR3 and drug tolerant) stages.

Combination drug screen

The combination drug screening platform has been described previously[14]. Briefly, the panel of screened compounds was comprised of 76 targeted agents directed against a broad range of biologic targets including regulators of growth factor and development signaling pathways, apoptosis, transcription and protein folding, and DNA damage. Cells were treated with vehicle or varying concentrations screen drugs (10,000-fold range) in the absence or presence of 1 μM WZ4002 for 72 hours and cell viability determined by CellTiter-Glo assay. Each dose response curve was normalized to cell viability of corresponding vehicle treated cells (with or without WZ4002). For each screen drug dose, a ΔE was calculated:

$$\Delta E = 1-(\text{Viability}(+WZ)/\text{Viability}(-WZ))$$

The means of the three lowest ΔE for all screen drugs were ranked, and screen drugs that scored 0.80 or lower in at least 2 of 3 cell lines were identified.

Data and Statistical Analysis

Data were analyzed using GraphPad Prism software (GraphPad Software). Unless otherwise specified, data displayed are mean and standard error. Pair-wise comparisons between groups (e.g., experimental versus control) were made using paired or unpaired T-tests as appropriate. For xenograft pharmacodynamic studies, unequal variance between groups was observed in a minority of cases, so Welch correction was performed for all comparisons. For all other experiments, variance between comparison groups was verified to be equivalent. P values below 0.05 were considered to be statistically significant.

References

1 Mok, T. *et al.* Gefitinib or carboplatin-paclitaxel in pulmonary adenocarcinoma. *N Engl J Med* **361**, 947-957 (2009).

2 Maemondo, M. *et al.* Gefitinib or chemotherapy for non-small-cell lung cancer with mutated EGFR. *N Engl J Med* **362**, 2380-2388, doi:362/25/2380 [pii] 10.1056/NEJMoa0909530 (2010).

3 Camidge, D. R., Pao, W. & Sequist, L. V. Acquired resistance to TKIs in solid tumours: learning from lung cancer. *Nat Rev Clin Oncol* **11**, 473-481, doi:10.1038/nrclinonc.2014.104 (2014).

4 Sequist, L. V. *et al.* Genotypic and histological evolution of lung cancers acquiring resistance to EGFR inhibitors. *Science translational medicine* **3**, 75ra26, doi:10.1126/scitranslmed.3002003 (2011).

5 Pao, W. *et al.* Acquired resistance of lung adenocarcinomas to gefitinib or erlotinib is associated with a second mutation in the EGFR kinase domain. *PLoS Med* **2**, e73, doi:10.1371/journal.pmed.0020073 (2005).

6 Engelman, J. A. *et al.* MET amplification leads to gefitinib resistance in lung cancer by activating ERBB3 signaling. *Science* **316**, 1039-1043, doi:10.1126/science.1141478 (2007).

7 Turke, A. B. *et al.* Preexistence and clonal selection of MET amplification in EGFR mutant NSCLC. *Cancer Cell* **17**, 77-88, doi:10.1016/j.ccr.2009.11.022 (2010).

8 Bhang, H. E. *et al.* Studying clonal dynamics in response to cancer therapy using high-complexity barcoding. *Nat Med*, doi:10.1038/nm.3841 (2015).

9 Su, K. Y. *et al.* Pretreatment epidermal growth factor receptor (EGFR) T790M mutation predicts shorter EGFR tyrosine kinase inhibitor response duration in patients with non-small-cell lung cancer. *J Clin Oncol* **30**, 433-440, doi:10.1200/JCO.2011.38.3224 (2012).

10 Ye, X. *et al.* High T790M detection rate in TKI-naive NSCLC with EGFR sensitive mutation: truth or artifact? *Journal of thoracic oncology : official publication of the International Association for the Study of Lung Cancer* **8**, 1118-1120, doi:10.1097/JTO.0b013e31829f691f (2013).

11 Sharma, S. V. *et al.* A chromatin-mediated reversible drug-tolerant state in cancer cell subpopulations. *Cell* **141**, 69-80, doi:10.1016/j.cell.2010.02.027 (2010).

12 Lee, H. J. *et al.* Drug resistance via feedback activation of Stat3 in oncogene-addicted cancer cells. *Cancer Cell* **26**, 207-221, doi:10.1016/j.ccr.2014.05.019 (2014).

13 Wilson, T. R. *et al.* Widespread potential for growth-factor-driven resistance to anticancer kinase inhibitors. *Nature* **487**, 505-509, doi:10.1038/nature11249 (2012).

14 Crystal, A. S. *et al.* Patient-derived models of acquired resistance can identify effective drug combinations for cancer. *Science*, doi:10.1126/science.1254721 (2014).

15 Zhou, W. *et al.* Novel mutant-selective EGFR kinase inhibitors against EGFR T790M. *Nature* **462**, 1070-1074, doi:10.1038/nature08622 (2009).

16 Hata, A. N., Engelman, J. A. & Faber, A. C. The BCL2 Family: Key Mediators of the Apoptotic Response to Targeted Anticancer Therapeutics. *Cancer Discov* **5**, 475-487, doi:10.1158/2159-8290.CD-15-0011 (2015).

17 Cragg, M. S., Kuroda, J., Puthalakath, H., Huang, D. C. & Strasser, A. Gefitinib-induced killing of NSCLC cell lines expressing mutant EGFR requires BIM and can be enhanced

by BH3 mimetics. *PLoS Med* **4**, 1681-1689; discussion 1690, doi:07-PLME-RA-0458 [pii]

10.1371/journal.pmed.0040316 (2007).

18 Costa, D. B. *et al.* BIM mediates EGFR tyrosine kinase inhibitor-induced apoptosis in lung cancers with oncogenic EGFR mutations. *PLoS Med* **4**, 1669-1679; discussion 1680, doi:07-PLME-RA-0425 [pii]

10.1371/journal.pmed.0040315 (2007).

19 Gong, Y. *et al.* Induction of BIM is essential for apoptosis triggered by EGFR kinase inhibitors in mutant EGFR-dependent lung adenocarcinomas. *PLoS Med* **4**, 1655-1668, doi:07-PLME-RA-0231 [pii]

10.1371/journal.pmed.0040294 (2007).

20 Faber, A. C. *et al.* BIM expression in treatment naïve cancers predicts responsiveness to kinase inhibitors. *Cancer Discov* **1**, 352-365, doi:10.1158/2159-8290.CD-11-0106 (2011).

21 Robasky, K., Lewis, N. E. & Church, G. M. The role of replicates for error mitigation in next-generation sequencing. *Nat Rev Genet* **15**, 56-62, doi:10.1038/nrg3655 (2014).

22 Hindson, B. J. *et al.* High-throughput droplet digital PCR system for absolute quantitation of DNA copy number. *Anal Chem* **83**, 8604-8610, doi:10.1021/ac202028g (2011).

23 Zheng, Z. *et al.* Anchored multiplex PCR for targeted next-generation sequencing. *Nat Med* **20**, 1479-1484, doi:10.1038/nm.3729 (2014).

24 Ohashi, K. *et al.* Lung cancers with acquired resistance to EGFR inhibitors occasionally harbor BRAF gene mutations but lack mutations in KRAS, NRAS, or MEK1. *Proc Natl Acad Sci U S A* **109**, E2127-2133, doi:10.1073/pnas.1203530109 (2012).

25 Eberlein, C. A. *et al.* Acquired Resistance to the Mutant-Selective EGFR Inhibitor AZD9291 Is Associated with Increased Dependence on RAS Signaling in Preclinical Models. *Cancer Res*, doi:10.1158/0008-5472.CAN-14-3167 (2015).

26 Piotrowska, Z. *et al.* Heterogeneity Underlies the Emergence of EGFR T790 Wild-Type Clones Following Treatment of T790M-Positive Cancers with a Third Generation EGFR Inhibitor. *Cancer Discov*, doi:10.1158/2159-8290.CD-15-0399 (2015).

27 Chmielecki, J. *et al.* Optimization of dosing for EGFR-mutant non-small cell lung cancer with evolutionary cancer modeling. *Science translational medicine* **3**, 90ra59, doi:10.1126/scitranslmed.3002356 (2011).

28 Tyson, D. R., Garbett, S. P., Frick, P. L. & Quaranta, V. Fractional proliferation: a method to deconvolve cell population dynamics from single-cell data. *Nat Methods* **9**, 923-928, doi:10.1038/nmeth.2138 (2012).

29 Janne, P. A. *et al.* AZD9291 in EGFR inhibitor-resistant non-small-cell lung cancer. *N Engl J Med* **372**, 1689-1699, doi:10.1056/NEJMoa1411817 (2015).

30 Sequist, L. V. *et al.* Rociletinib in EGFR-mutated non-small-cell lung cancer. *N Engl J Med* **372**, 1700-1709, doi:10.1056/NEJMoa1413654 (2015).

31 Cross, D. A. *et al.* AZD9291, an irreversible EGFR TKI, overcomes T790M-mediated resistance to EGFR inhibitors in lung cancer. *Cancer Discov* **4**, 1046-1061, doi:10.1158/2159-8290.CD-14-0337 (2014).

32 Cragg, M. S. *et al.* Treatment of B-RAF mutant human tumor cells with a MEK inhibitor requires Bim and is enhanced by a BH3 mimetic. *J Clin Invest* **118**, 3651-3659, doi:10.1172/JCI35437 (2008).

33 Corcoran, R. B. *et al.* Synthetic Lethal Interaction of Combined BCL-XL and MEK Inhibition Promotes Tumor Regressions in KRAS Mutant Cancer Models. *Cancer Cell* **23**, 121-128, doi:10.1016/j.ccr.2012.11.007 (2013).

34 McGranahan, N. & Swanton, C. Biological and therapeutic impact of intratumor heterogeneity in cancer evolution. *Cancer Cell* **27**, 15-26, doi:10.1016/j.ccell.2014.12.001 (2015).

35 de Bruin, E. C. *et al.* Spatial and temporal diversity in genomic instability processes defines lung cancer evolution. *Science* **346**, 251-256, doi:10.1126/science.1253462 (2014).

36 Misale, S., Di Nicolantonio, F., Sartore-Bianchi, A., Siena, S. & Bardelli, A. Resistance to anti-EGFR therapy in colorectal cancer: from heterogeneity to convergent evolution. *Cancer Discov* **4**, 1269-1280, doi:10.1158/2159-8290.CD-14-0462 (2014).

37 Maheswaran, S. *et al.* Detection of mutations in EGFR in circulating lung-cancer cells. *N Engl J Med* **359**, 366-377, doi:10.1056/NEJMoa0800668 (2008).

38 Byers, L. A. *et al.* An epithelial-mesenchymal transition gene signature predicts resistance to EGFR and PI3K inhibitors and identifies Axl as a therapeutic target for overcoming EGFR inhibitor resistance. *Clin Cancer Res* **19**, 279-290, doi:10.1158/1078-0432.CCR-12-1558 (2013).

39 Hirata, E. *et al.* Intravital Imaging Reveals How BRAF Inhibition Generates Drug-Tolerant Microenvironments with High Integrin beta1/FAK Signaling. *Cancer Cell* **27**, 574-588, doi:10.1016/j.ccell.2015.03.008 (2015).

40 Niederst, M. J. *et al.* RB loss in resistant EGFR mutant lung adenocarcinomas that transform to small-cell lung cancer. *Nat Commun* **6**, 6377, doi:10.1038/ncomms7377 (2015).

41 Misale, S. *et al.* Blockade of EGFR and MEK intercepts heterogeneous mechanisms of acquired resistance to anti-EGFR therapies in colorectal cancer. *Science translational medicine* **6**, 224ra226, doi:10.1126/scitranslmed.3007947 (2014).

42 Dias-Santagata, D. *et al.* Rapid targeted mutational analysis of human tumours: a clinical platform to guide personalized cancer medicine. *EMBO Mol Med* **2**, 146-158, doi:10.1002/emmm.201000070 (2010).

43 Hata, A. N. *et al.* Failure to induce apoptosis via BCL-2 family proteins underlies lack of efficacy of combined MEK and PI3K inhibitors for KRAS-mutant lung cancers. *Cancer Res* **74**, 3146-3156, doi:10.1158/0008-5472.CAN-13-3728 (2014).

44 Kunkel, T. A. & Bebenek, K. DNA replication fidelity. *Annu Rev Biochem* **69**, 497-529, doi:10.1146/annurev.biochem.69.1.497 (2000).

45 Oller, A. R., Rastogi, P., Morgenthaler, S. & Thilly, W. G. A statistical model to estimate variance in long term-low dose mutation assays: testing of the model in a human lymphoblastoid mutation assay. *Mutat Res* **216**, 149-161 (1989).

46 Lynch, M. Rate, molecular spectrum, and consequences of human mutation. *Proc Natl Acad Sci U S A* **107**, 961-968, doi:10.1073/pnas.0912629107 (2010).

47 Alexandrov, L. B. *et al.* Signatures of mutational processes in human cancer. *Nature* **500**, 415-421, doi:10.1038/nature12477 (2013).

48 Lawrence, M. S. *et al.* Mutational heterogeneity in cancer and the search for new cancer-associated genes. *Nature* **499**, 214-218, doi:10.1038/nature12213 (2013).

49 Dobin, A. *et al.* STAR: ultrafast universal RNA-seq aligner. *Bioinformatics* **29**, 15-21, doi:10.1093/bioinformatics/bts635 (2013).

50 Anders, S., Pyl, P. T. & Huber, W. HTSeq--a Python framework to work with high-throughput sequencing data. *Bioinformatics* **31**, 166-169, doi:10.1093/bioinformatics/btu638 (2015).

51 Robinson, M. D., McCarthy, D. J. & Smyth, G. K. edgeR: a Bioconductor package for differential expression analysis of digital gene expression data. *Bioinformatics* **26**, 139-140, doi:10.1093/bioinformatics/btp616 (2010).

52 Subramanian, A. *et al.* Gene set enrichment analysis: a knowledge-based approach for interpreting genome-wide expression profiles. *Proc Natl Acad Sci U S A* **102**, 15545-15550, doi:10.1073/pnas.0506580102 (2005).

53 Mootha, V. K. *et al.* PGC-1alpha-responsive genes involved in oxidative phosphorylation are coordinately downregulated in human diabetes. *Nat Genet* **34**, 267-273, doi:10.1038/ng1180 (2003).

Acknowledgements

We thank Cyril Benes and all members of the Engelman and Benes Lab for helpful discussions and feedback. This study was funded by support from the NIH R01CA137008 (J.A.E.), the Department of Defense (L.V.S. and J.A.E.), LunGevity (L.V.S. and J.A.E.), Uniting Against Lung Cancer (A.N.H. and M.J.N.), Conquer Cancer Foundation of ASCO (A.N.H.), Lung Cancer Research Foundation (M.J.N), Targeting a Cure for Lung Cancer, and Be a Piece of the Solution.

Author Contributions

A.N.H., M.J.N. and J.A.E. designed the study, analyzed the data and wrote the paper. A.N.H, M.J.N., H.L.A, M.G.C., H.M, H.H., F.M.S, L.J.D. performed cell line and biochemical studies. M.G.C. and C.C. performed tumor xenograft studies. E.L., A.K., D.L. generated the patient derived cell lines. H.C.B, V.K.R., C.L.K., D.A.R., F.S performed analysis of barcode analysis. Y.M., G.G. performed mathematical modeling of T790M evolution. F.J, R.S. performed RNA-Seq analysis. A.C. performed combination drug screening. G.S., A.J.I. and A.B., performed genotyping analysis. S.R. performed mathematical modeling of emergence of resistant clones. A.F was involved with study design. L.V.S. and Z.P. provided EGFR mutant patient samples. A.N.H and M.J.N. contributed equally to the study. All authors discussed the results and commented on the manuscript

Author Information

The authors declare competing financial interests: J.A.E. is a consultant for Novartis, Sanofi, Genentech, Clovis and Astra Zeneca; owns equity in Gatekeeper Pharmaceuticals, which has interest in T790M inhibitors; has research agreements with Novartis and Astra Zeneca. Z.P. has provided consulting services for Clovis Oncology. A.N.H. has provided consulting services for Amgen. L.V.S. has provided uncompensated consulting services to Clovis Oncology, AstraZeneca, Novartis, Boehringer-Ingelheim, Merrimack Pharmaceuticals, Genentech and Taiho Pharmaceuticals. Correspondence and requests for materials should be addressed to J.A.E (jengelman@mgh.harvard.edu).

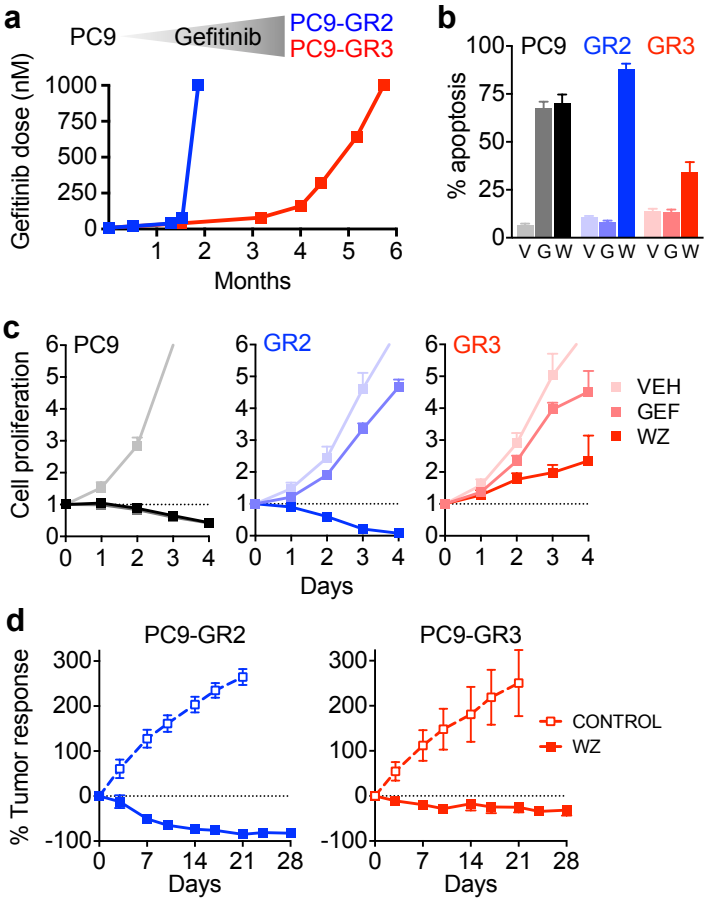
a
PC9
Gefitinib
PC9-GR2
PC9-GR3
Gefitinib dose (nM)
1000
750
500
250
0
1 2 3 4 5 6
Months
b
100
75
50
25
0
% apoptosis
PC9 GR2 GR3
V G W V G W V G W
c
PC9
GR2
GR3
Cell proliferation
6
5
4
3
2
1
0
0 1 2 3 4
Days
VEH
GEF
WZ
d
PC9-GR2
PC9-GR3
% Tumor response
300
200
100
0
-100
0 7 14 21 28
Days
CONTROL
WZ

Figure 1

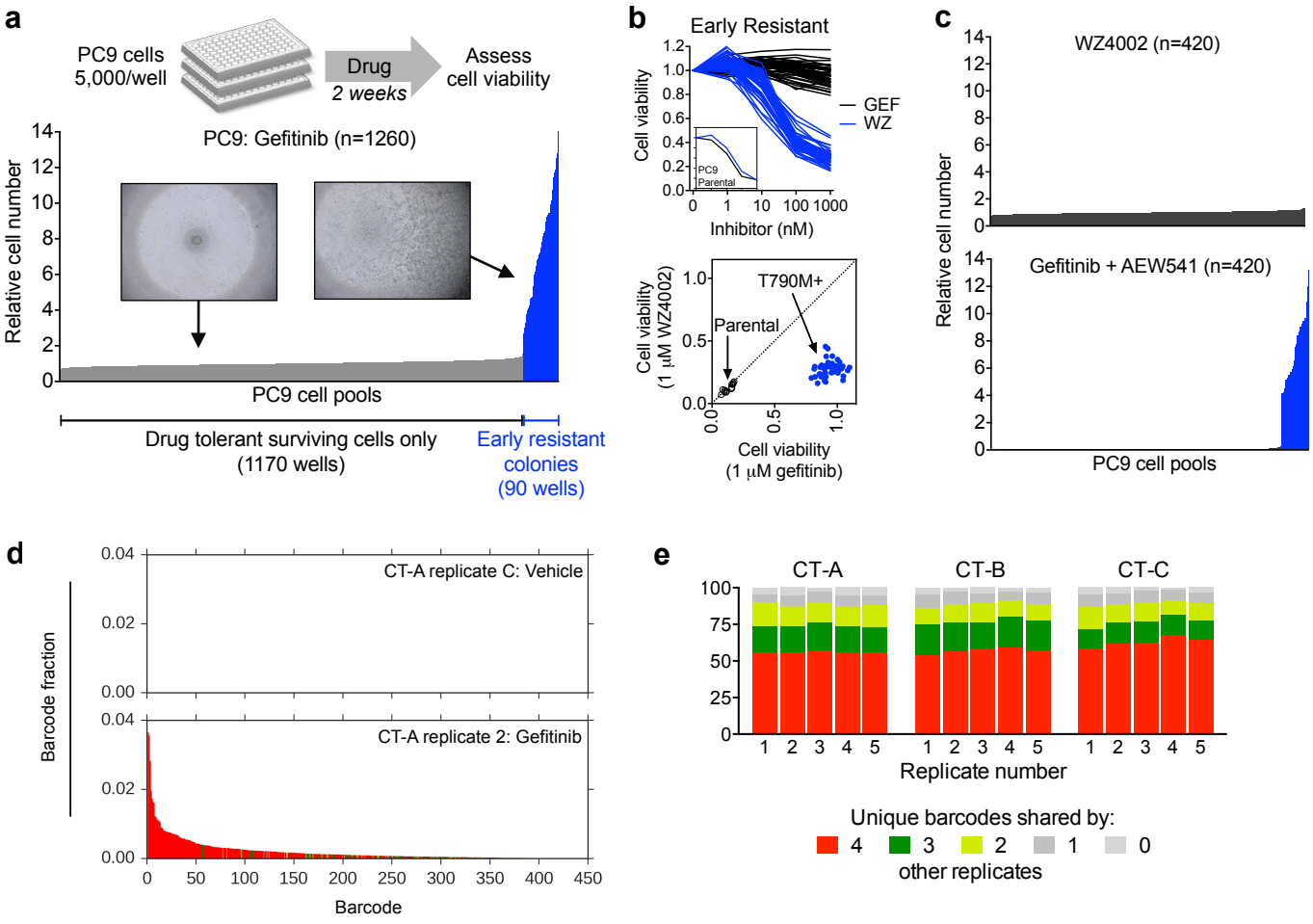
a
PC9 cells
5,000/well
Drug
2 weeks
Assess
cell viability
PC9: Gefitinib (n=1260)
Relative cell number
PC9 cell pools
Drug tolerant surviving cells only
(1170 wells)
Early resistant
colonies
(90 wells)
b
Early Resistant
Cell viability
GEF
WZ
PC9
Parental
Inhibitor (nM)
Cell viability
(1 μM WZ4002)
T790M+
Parental
Cell viability
(1 μM gefitinib)
c
WZ4002 (n=420)
Relative cell number
Gefitinib + AEW541 (n=420)
PC9 cell pools
d
Barcode fraction
CT-A replicate C: Vehicle
CT-A replicate 2: Gefitinib
Barcode
e
CT-A
CT-B
CT-C
Replicate number
Unique barcodes shared by:
4
3
2
1
0
other replicates

Figure 2

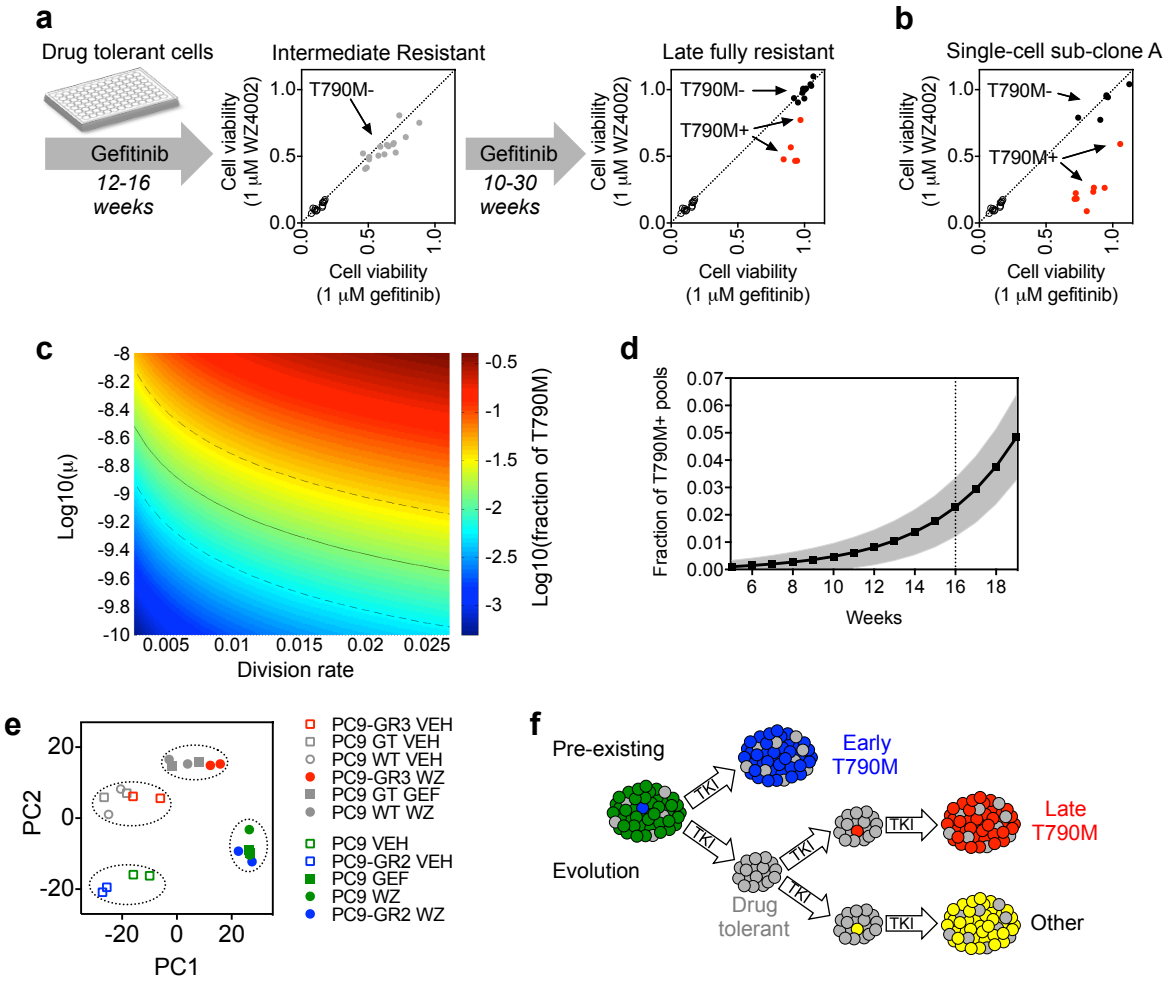
a
Drug tolerant cells
Gefitinib
12-16 weeks
Intermediate Resistant
Cell viability (1 μM WZ4002)
T790M-
Cell viability (1 μM gefitinib)
Gefitinib
10-30 weeks
Late fully resistant
T790M-
T790M+
b
Single-cell sub-clone A
c
Log10(μ)
Division rate
Log10(fraction of T790M)
d
Fraction of T790M+ pools
Weeks
e
PC2
PC1
PC9-GR3 VEH
PC9 GT VEH
PC9 WT VEH
PC9-GR3 WZ
PC9 GT GEF
PC9 WT WZ
PC9 VEH
PC9-GR2 VEH
PC9 GEF
PC9 WZ
PC9-GR2 WZ
f
Pre-existing
Early T790M
TKI
Evolution
Drug tolerant
Late T790M
Other

Figure 3

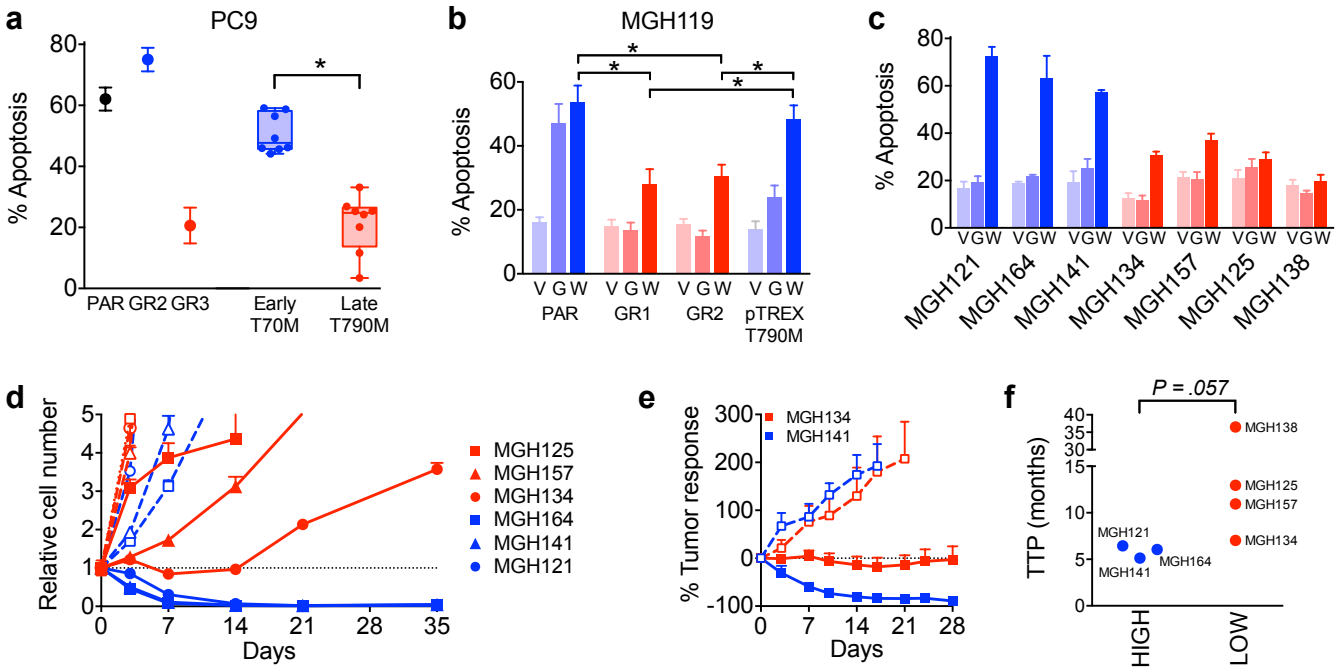
a
PC9
% Apoptosis
PAR GR2 GR3
Early T70M
Late T790M
b
MGH119
% Apoptosis
V G W
PAR
GR1
GR2
pTREX T790M
c
% Apoptosis
MGH121
MGH164
MGH141
MGH134
MGH157
MGH125
MGH138
d
Relative cell number
Days
MGH125
MGH157
MGH134
MGH164
MGH141
MGH121
e
% Tumor response
MGH134
MGH141
Days
f
P = .057
TTP (months)
MGH138
MGH125
MGH157
MGH134
MGH121
MGH164
MGH141
HIGH
LOW

Figure 4

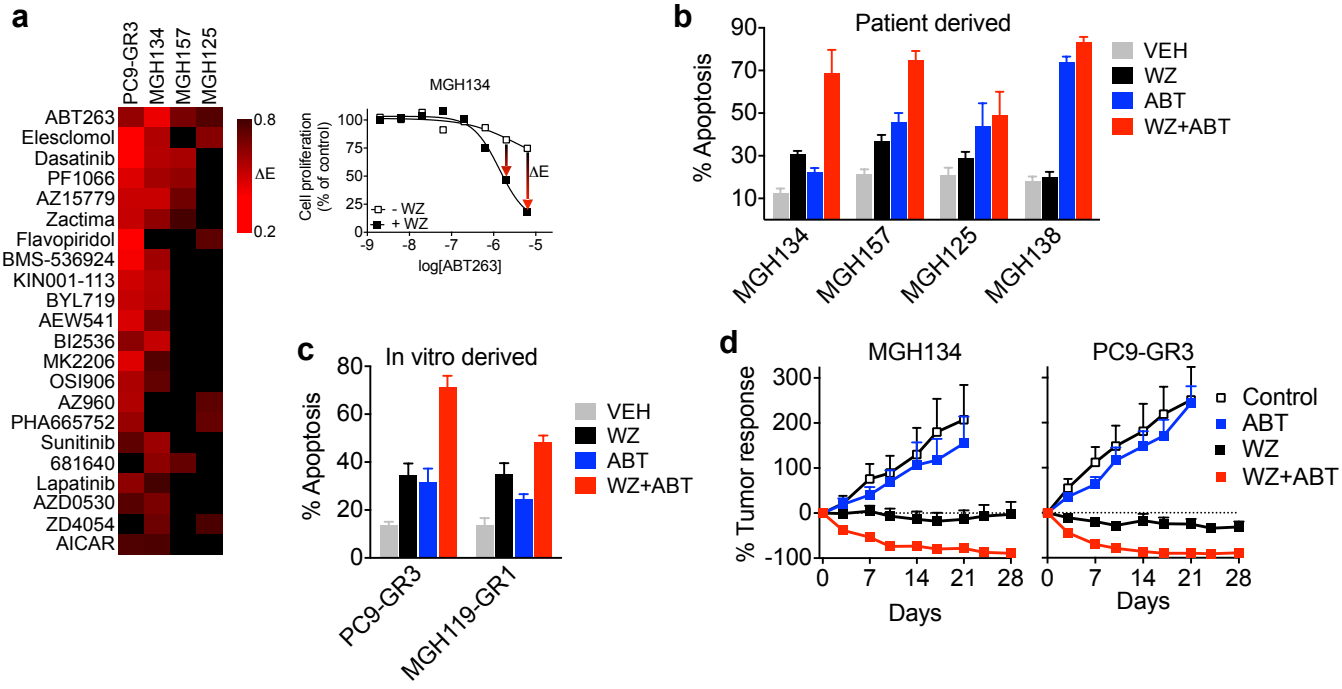
a
PC9-GR3
MGH134
MGH157
MGH125
ABT263
Elesclomol
Dasatinib
PF1066
AZ15779
Zactima
Flavopiridol
BMS-536924
KIN001-113
BYL719
AEW541
BI2536
MK2206
OSI906
AZ960
PHA665752
Sunitinib
681640
Lapatinib
AZD0530
ZD4054
AICAR
0.8
ΔE
0.2
MGH134
Cell proliferation (% of control)
- WZ
+ WZ
ΔE
log[ABT263]
b
Patient derived
% Apoptosis
VEH
WZ
ABT
WZ+ABT
MGH134
MGH157
MGH125
MGH138
c
In vitro derived
% Apoptosis
VEH
WZ
ABT
WZ+ABT
PC9-GR3
MGH119-GR1
d
MGH134
PC9-GR3
% Tumor response
Control
ABT
WZ
WZ+ABT
Days
Days

Figure 5